

UNCLASSIFIED



Australian Government

Department of Defence
Science and Technology

Mechanical Testing of Helicopter Underslung Load Equipment (HUSLE) Roundslings

*Kate Bourne, Keith Muller, Carl Mouser, Bruce Grigson,
Jim Nicholls and Thuan Truong*

Aerospace Division
Defence Science and Technology Group

DST-Group-TN-1614

ABSTRACT

Following on from preliminary testing in 2013, mechanical testing of the Helicopter Underslung Load Equipment (HUSLE) roundslings was undertaken in support of slung load simulation model development. DST Group conducted tensile and dynamic testing on an expired HUSLE assembly in order to identify the mechanical properties of the roundslings.

RELEASE LIMITATION

Approved for public release

UNCLASSIFIED

UNCLASSIFIED

Produced by

*Aerospace Division
Defence Science and Technology Group
506 Lorimer Street
Fishermans Bend VIC 3207*

Telephone: 1300 333 362

*© Commonwealth of Australia 2017
April 2017
AR-016-835*

APPROVED FOR PUBLIC RELEASE

UNCLASSIFIED

UNCLASSIFIED

Mechanical Testing of Helicopter Underslung Load Equipment (HUSLE) Roundslings

Executive Summary

Following on from preliminary testing in 2013, mechanical testing of the Helicopter Underslung Load Equipment (HUSLE) roundslings was undertaken in support of slung load simulation model development. To ensure that the simulation code appropriately replicates the physics of slung load operations, the mechanical properties of the slung load equipment must be included.

DST Group conducted tensile and dynamic testing on an expired HUSLE assembly in order to identify the mechanical properties of the roundslings. Given the tested equipment was unserviceable, the results presented here are considered appropriate for improving the fidelity of the simulation, but **cannot** be interpreted as suitable for application in an operational context. If data is required for direct application to load clearance activities, destructive testing of a serviceable HUSLE assembly would need to be undertaken.

UNCLASSIFIED

UNCLASSIFIED

This page is intentionally blank.

UNCLASSIFIED

Contents

1. INTRODUCTION.....	1
2. HUSLE SPECIFICATIONS	2
3. STATIC TESTING.....	4
3.1 Test Setup and Procedure.....	4
3.2 Results.....	4
4. DYNAMIC TESTING	6
4.1 Test Setup and Procedure.....	6
4.2 Instrumentation.....	7
4.3 Motion Analysis.....	9
4.4 Test Cases	11
4.5 Damping Ratio from Logarithmic Decrement	11
4.5.1 Analysis Method.....	14
4.5.2 Accelerometer Data.....	14
4.5.3 Motion Analysis Data	16
5. DISCUSSION	19
6. LIMITATIONS AND CAVEATS.....	19
7. REFERENCES	20
APPENDIX A DAMPED FREQUENCY FROM ACCELEROMETER AND LOAD CELL DATA	21
APPENDIX B LOAD CELL AND ACCELEROMETER DATA - RESPONSE PROFILES	23
B.1 Run01: Suspended Weight 560 kg, Preload total 1050 kg.....	23
B.2 Run02: Suspended weight 560 kg, Preload total 1050 kg	25
B.3 Run03: Suspended weight 1615 kg, Preload total 2130 kg	26
B.4 Run04: Suspended weight 2670 kg, Preload total 3220 kg	28
B.5 Run05: Suspended weight 2685 kg, Preload total 3205 kg	29
B.6 Run06: Suspended weight 3763 kg, Preload total 4290 kg	31
B.7 Run07: Suspended weight 3770 kg, Preload total 4280 kg	32
B.8 Run08: Suspended weight 550 kg, Preload total 1045 kg	34
B.9 Run09: Suspended weight 552 kg, Preload total 970 kg	35

APPENDIX C DISPLACEMENT DERIVED FROM ACCELEROMETER DATA 37

C.1 Run01: Suspended Weight 560kg, Preload total 1050kg..... 37
C.2 Run02: Suspended weight 560 kg, Preload total 1050 kg 38
C.3 Run03: Suspended weight 1615 kg, Preload total 2130 kg 38
C.4 Run04: Suspended weight 2670 kg, Preload total 3220 kg 39
C.5 Run05: Suspended weight 2685 kg, Preload total 3205 kg 39
C.6 Run06: Suspended weight 3763 kg, Preload total 4290 kg 40
C.7 Run07: Suspended weight 3770 kg, Preload total 4280 kg 40
C.8 Run08: Suspended weight 550 kg, Preload total 1045 kg 41
C.9 Run09: Suspended weight 552 kg, Preload total 970 kg 41

APPENDIX D MOTION ANALYSIS DATA..... 43

D.1 Run01: Suspended Weight 560kg, Preload total 1050kg..... 43
D.2 Run02: Suspended weight 560 kg, Preload total 1050 kg 44
D.3 Run04: Suspended weight 2670 kg, Preload total 3220 kg 45
D.4 Run05: Suspended weight 2685 kg, Preload total 3205 kg 46
D.5 Run06: Suspended weight 3763 kg, Preload total 4290 kg 47
D.6 Run07: Suspended weight 3770 kg, Preload total 4280 kg 48
D.7 Run08: Suspended weight 550 kg, Preload total 1045 kg 49
D.8 Run09: Suspended weight 552 kg, Preload total 970 kg 50

Abbreviations

AMTDU	Air Movements Training and Development Unit
AVT	Advanced VTOL Technologies
DST Group	Defence Science and Technology Group
HUSLE	Helicopter Underslung Load Equipment
OEM	Original Equipment Manufacturer

UNCLASSIFIED

DST-Group-TN-1614

This page is intentionally blank.

UNCLASSIFIED

1. Introduction

The Defence Science and Technology (DST) Group contracted development of a helicopter slung load simulation tool to Advanced VTOL Technologies (AVT) to meet the requirements of the Air Movements Training and Development Unit (AMTDU). AMTDU are responsible for clearance of all externally slung loads, a process which includes engineering analysis, static testing and flight testing. The end use of the software is to aid in the initial stages of analysis and to identify potential risks during flight test.

In order to provide simulations of sufficient fidelity, pertinent data must be gathered to suitably characterise the mechanical and material properties of the slung load system. Although original test and qualification data for the AmSafe Helicopter UnderSlung Load Equipment (HUSLE) was provided by the Original Equipment Manufacturer (OEM) [1], the full range of parameters required for simulation was not available.

Preliminary testing was undertaken in 2013 [2] but AMTDU required that the HUSLE assembly remain in serviceable condition. Consequently the testing was conservatively limited to loads well within the OEM specification for maximum restraining weight. The results presented here were conducted on a HUSLE assembly that had been decommissioned following expiry of its shelf-life¹, which enabled a more thorough test regime to be pursued. Given the tested equipment was unserviceable, the results presented here are considered appropriate for improving the fidelity of the simulation, but **cannot** be interpreted as suitable for application in an operational context. If data is required for direct application to load clearance activities, destructive testing of a serviceable HUSLE assembly would need to be undertaken.

¹ The HUSLE assemblies have a limited service life based on the date of first use.

2. HUSLE Specifications

The 4-legged HUSLE² comprises the components outlined in Figure 1. Each leg is made up of roundslings³, half links, chains and shortening clutches. Two masterlinks provide a connection point between the sling legs and helicopter cargo hook. Specifications are provided in Table 1. All information is taken from the AmSafe user manual [3].

Table 1: 4-legged HUSLE Specifications

Overall length	6550 mm
Material	
Round sling	Polyester
Metalware	Forged steel
Maximum Load Capacity	
Angle of legs: 50°	11 500 kg (25 350 lb)
Angle of legs: 80°	9 550 kg (21 050 lb)

² AmSafe part number HU30-0151300: Sling, Multiple-Leg, Heavy Duty, 4-Legged.

³ Roundslings are webbing sleeves with an internal polyester core, of circular cross-section.

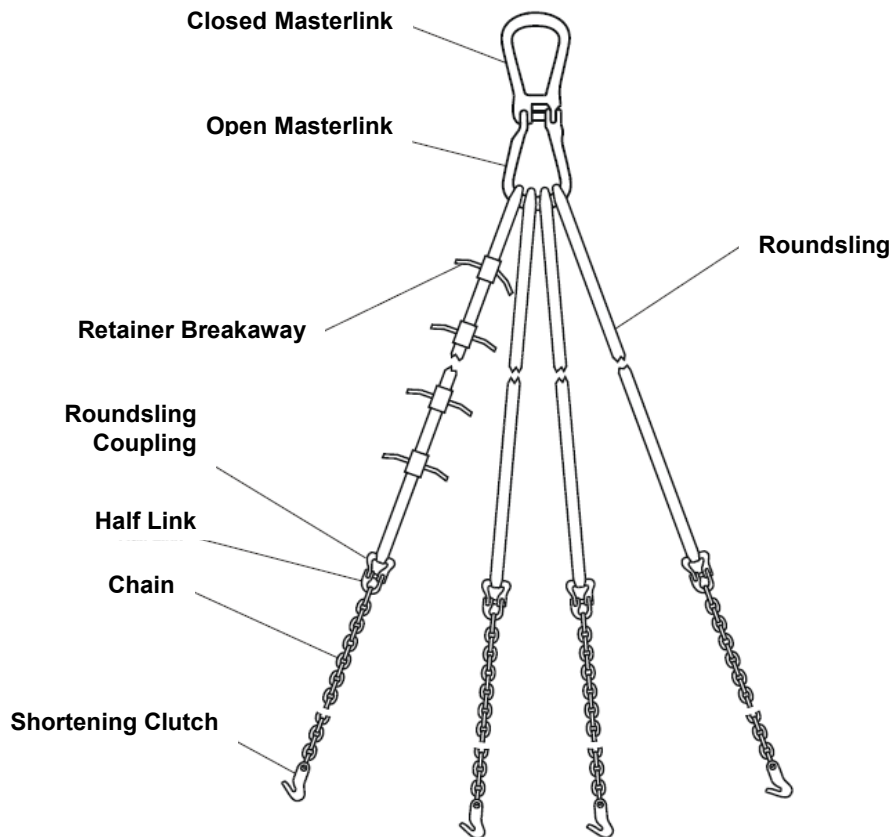


Figure 1: 4-legged HUSLE (image taken from [3])

The following is provided in the AmSafe user manual in relation to operating limitations:

Operating Limitations

The 4-Legged Multiple-Leg Sling has the following limitations:

1. The maximum load capacity is only valid when all the legs of the Multiple-Leg Sling are being used and each leg has an equal share of the load. If less than four legs are being used to lift a load then the maximum load capacity is reduced proportionately.
2. The maximum loads capacity is only valid if the angle between the legs does not exceed the specified angle.
3. When the angle of the legs is between 1° and 50° , the Multiple-Leg Sling has a maximum restraining weight of 11 500 kg (25 350 lb)
4. When the angle of the legs is between 51° and 80° , the Multiple-Leg Sling has a maximum restraining weight of 9550 kg (21 050 lb)
5. It must not be used in temperatures less than -40°C (-40°F) or more than $+66^{\circ}\text{C}$ ($+150^{\circ}\text{F}$)

3. Static Testing

3.1 Test Setup and Procedure

Static testing was completed within the Fatigue Laboratory at DST Group (Melbourne) using the Longbed Horizontal Tensile Testing Machine⁴, as shown in Figure 2. A single HUSLE roundsling was fitted in the machine, with one end connected via the masterlink and the other via the hammer lock that usually coupled the roundsling to the chain. The applied load was incrementally increased until failure.



Figure 2: HUSLE installed in the Longbed Horizontal Tensile Testing Machine

3.2 Results

Test results of the tensile test are presented in Figure 3, showing the sling displacement with applied load. The maximum elongation of the roundsling was 228 mm when the master lock failed at 164 kN. The pin of the master lock assembly failed first leading to failure of the ring that was attached to the rig. Images of the failed master lock are presented in Figure 4.

⁴ 200kN Magnetic Flux Leakage, Type LZED.

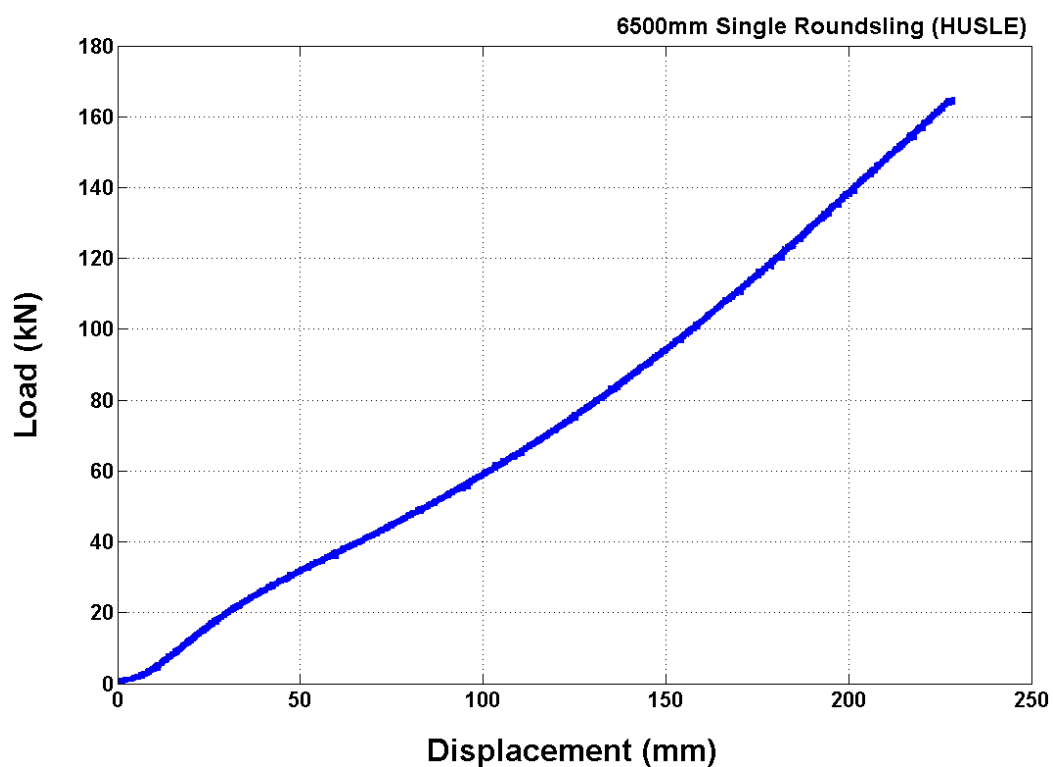


Figure 3: Tensile test result for single HUSLE roundsling

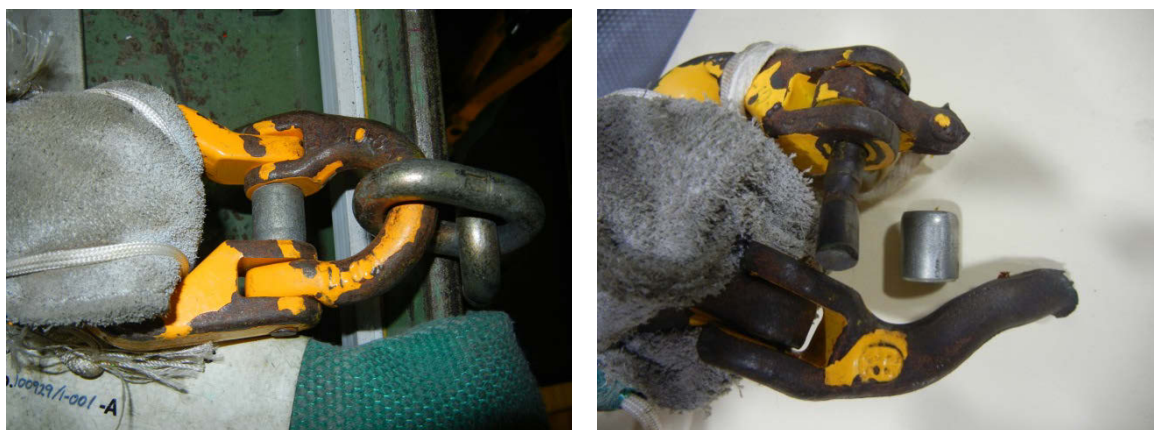


Figure 4: Roundsling coupling in working order (left) and post-failure (right)

The tensile test peak loading of 164 kN equated to a restraining weight 5.8 times greater than the maximum safe load specified by the OEM.

4. Dynamic Testing

4.1 Test Setup and Procedure

In order to determine the dynamic stiffness of key HUSLE components, the OEM implemented a test procedure that generated vertical oscillation in the sling assembly[1]. The same approach was adopted by DST Group in order to determine the rebound decay and hence the logarithmic decrement of the roundslings under varying loads. The test rig comprised a steel support frame that suspended the roundsling assembly above a carriage that could be loaded with crane weights, as shown in Figure 5. The sling and carriage assembly was pre-loaded via a pulley system connected to a remote release hook. A tension load of 500 kg was applied prior to release, which resulted in vertical oscillation of the roundsling.



Figure 5 HUSLE test rig

4.2 Instrumentation

Accelerometers were installed on the top beam of the gantry frame and on the top beam of the carriage. The accelerometers were placed in-line with the HUSLE, with the accelerometers on the gantry measuring in the Z-direction (extension in the HUSLE) only. The accelerometers on the carriage were tri-axial accelerometers and the acceleration in all three directions was recorded. The location and specification of the accelerometers are provided in *Table 2* and *Figure 6*. Two accelerometers were installed in each location so as to provide redundancy in the instrumentation.

Table 2: Instrumentation location and details

Location	Channel name	Type	Direction	Calibration factor
Gantry frame	Upper_A	Accelerometer	Z	9.61 mV/g
	Upper_B	Accelerometer	Z	10.06 mV/g
	Load_A	Load cell	Z	0.19316 mV/kN
	Load_B	Load cell	Z	0.19231 mV/kN
Carriage	Lwr_sth:+X	Accelerometer	X	105.6 mV/g
	Lwr_sth_+Y	Accelerometer	Y	104.5 mV/g
	Lwr_sth:+Z	Accelerometer	Z	102.6 mV/g
	Lwr_nrth:+X	Accelerometer	X	102.0 mV/g
	Lwr_nrth_+Y	Accelerometer	Y	99.15 mV/g
	Lwr_nrth:+Z	Accelerometer	Z	102.6 mV/g

An LMS SCADAS system was used to measure and store the data from the accelerometers and load cells. The system was configured with a sample rate of 1024 samples per second and all channels were acquired simultaneously.

Initial assessments of the data showed that the load cells were affected by a 50 Hz powerline pickup. The source of this could not be identified and as the frequency of interest was much lower than 50 HZ, testing continued. A 40 Hz low pass filter was used to post-process all the data so as to remove the 50 Hz signal from the data. Even though the accelerometers were not affected by the 50 Hz noise the filter was applied to the accelerometers signal to maintain consistency in the signal processing.

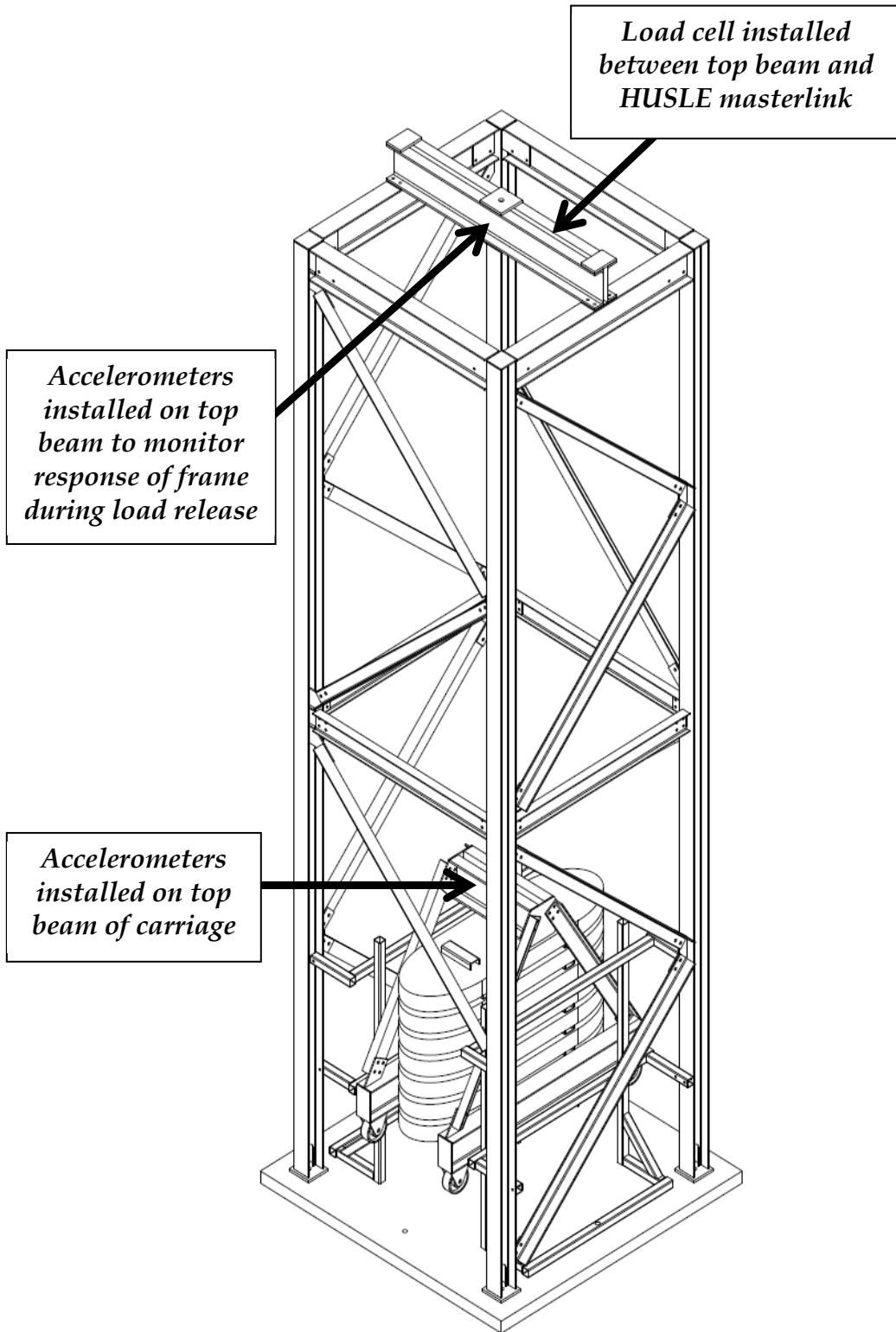


Figure 6: Location of installed instrumentation

4.3 Motion Analysis

A Photron SA5 monochrome high speed video camera was used to record the oscillation of the sling assembly by imaging a marker at 500 frames per second, which was located on one side of the apex of the load carriage. The camera was placed perpendicular to the field of view with the sensor parallel to the plane of motion to eliminate perspective distortion. A field of view of 512 pixels horizontally by 1025 pixels vertically was recorded for each event. Motion analysis software was then used to analyse the position of a marker in a calibrated 2D space.

Presented in Figure 7 is a screen shot from the motion analysis software. Marked in red is the point cloud resulting from automated tracking of the centre of gravity of the marker. The point cloud represents the range of frames measured for the current event superimposed on one frame.

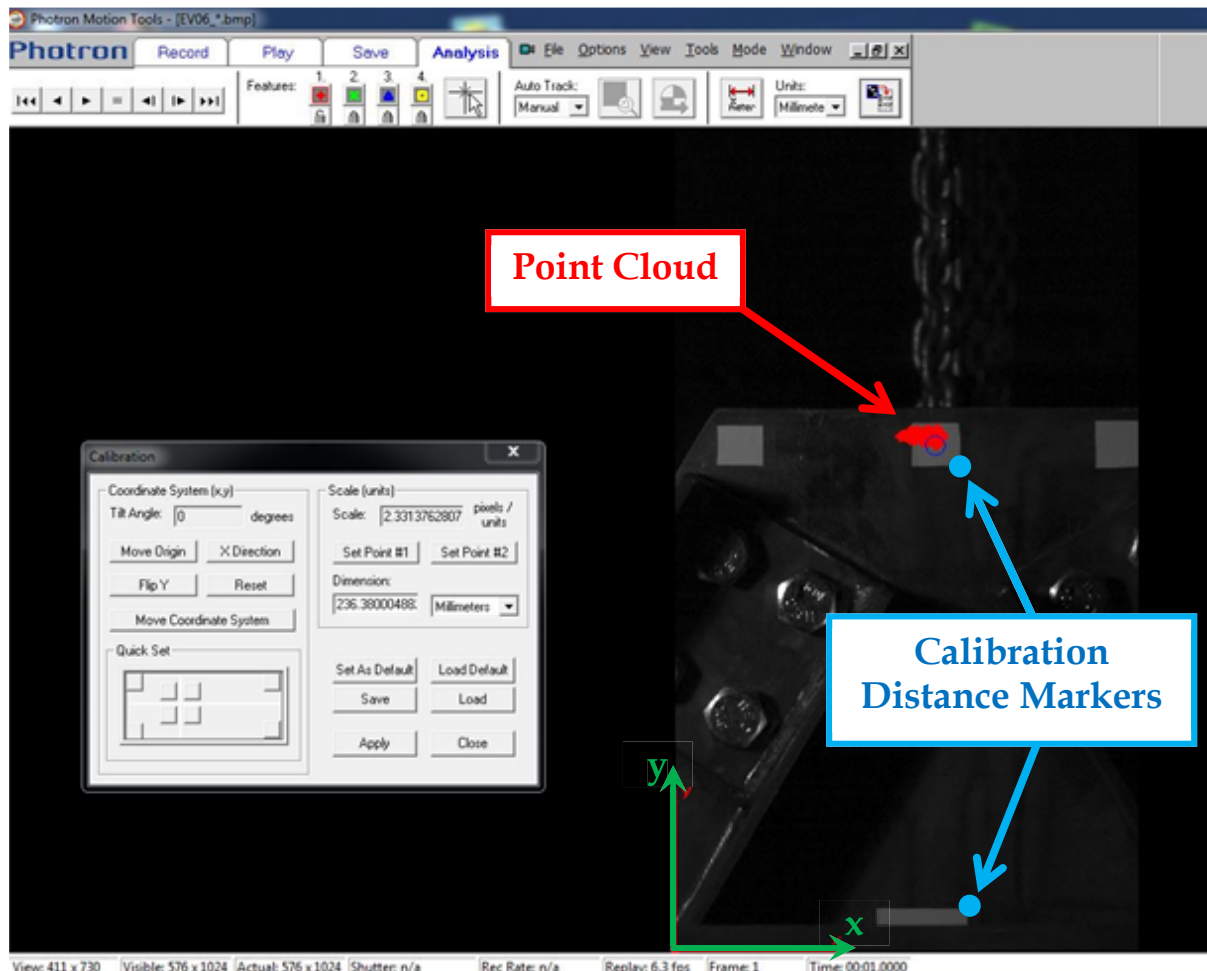


Figure 7: Screen shot from motion analysis software showing key values

The two blue dots show the corners of white markers used to provide the calibration distance for the analysis. The calibration distance was measured in situ using a digital Vernier calliper and provided as an input to the motion analysis software to determine the spatial resolution of the image (pixels per millimetre). From this, the displacement of the load carriage could be determined in real-world units. The coordinate system was set to locate the zero XY value or origin in the bottom left hand corner of the image, as per the green axes.

Figure 8 shows a close-up view of a point cloud generated from analysis of the movement of the centre of gravity of the marker over the range of frames analysed for a single event. The starting location is identified by the open blue circle. The displacement data calculated from the motion analysis was then exported for further analysis, as outlined in Section 4.5.

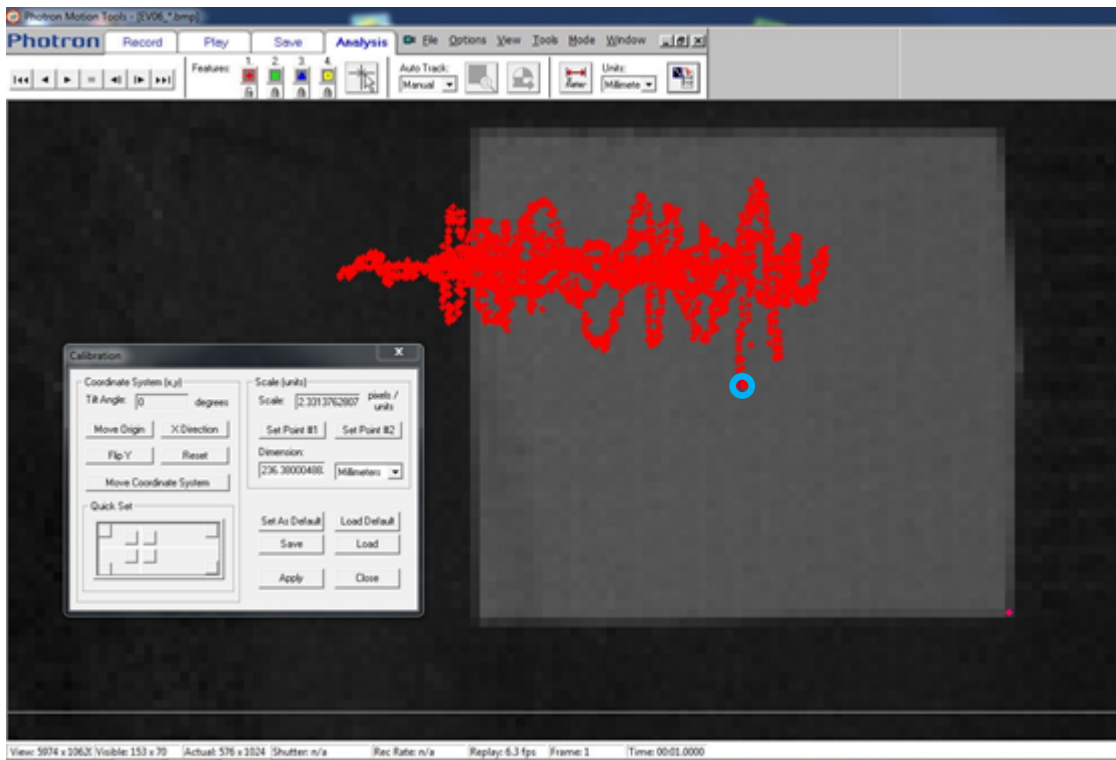


Figure 8: Point cloud generated by motion analysis showing load displacement over a single run. Initial position marked by open blue circle.

4.4 Test Cases

Provided in Table 3 are the details of each test case. To assist in carriage alignment small weights were added to the suspended load, which resulted in minor variation in the suspended weight and preload totals for test points that were otherwise in the same test configuration (i.e. Run02/03, Run04/05, Run06/07, Run01/08/09).

From preliminary testing of the gantry and release mechanisms it was determined that the gantry was of sufficient stiffness so as to negate the need for additional signal processing to account for the gantry displacement response under load.

Table 3: Details of each test point

Run	Suspended Weight (kgf)	Preload Total (kgf)
01	560	1050
02	1610	2145
03	1610	2130
04	2670	3220
05	2685	3205
06	3763	4290
07	3770	4280
08	550	1045
09	550	970

4.5 Damping Ratio from Logarithmic Decrement

One of the key parameters required by the slung load simulation software relates to the damping properties of the HUSLE roundslings. In order to estimate the damping ratio of the roundslings, the logarithmic decrement (δ) [4] can be measured by experiment. The logarithmic decrement represents the rate at which the amplitude of a free damped vibration decreases and is defined as the natural log of the ratio of the amplitudes of any two successive peaks, as shown in Figure 9:

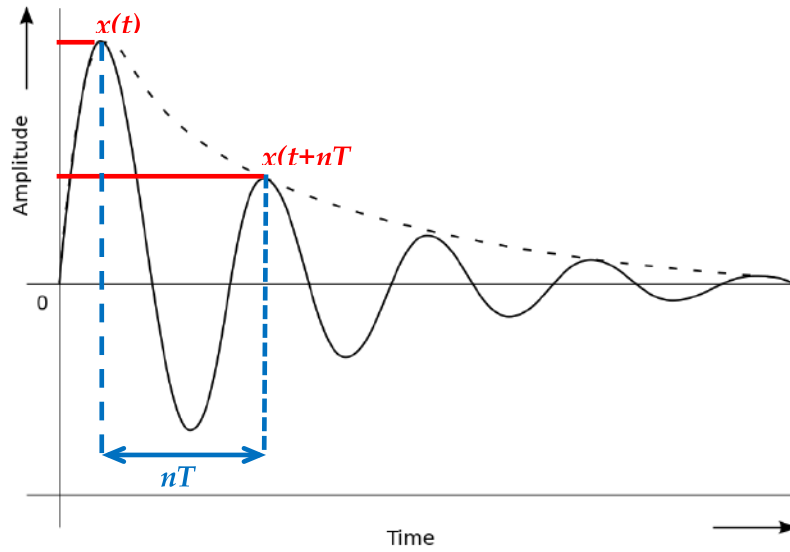


Figure 9: Free damped vibration

where,

$$\delta = \frac{1}{n} \ln \frac{x(t)}{x(t+nT)} \quad (1)$$

The damping ratio can then be calculated from the logarithmic decrement:

$$\zeta = \frac{1}{\sqrt{1 + \left(\frac{2\pi}{\delta}\right)^2}} \quad (2)$$

The natural frequency, ω_n , of the vibration of the system can then be calculated from the damped natural frequency, ω_d , and the damping ratio:

$$\omega_d = \frac{2\pi}{T} \quad (3)$$

$$\omega_n = \frac{\omega_d}{\sqrt{1 - \zeta^2}} \quad (4)$$

Shown in Figure 10 and Figure 11 are example results of the data obtained from the load cell and accelerometers. From this data the damped natural frequency (ω_d) of each run was calculated. The data presented in Table 4 are the results averaged between data from the load cell (bridge A) and the carriage accelerometer (North, z-direction). A full list of the frequency values calculated for each run is presented in Appendix A and the response profiles recorded by the load cell and accelerometers is provided in Appendix B.

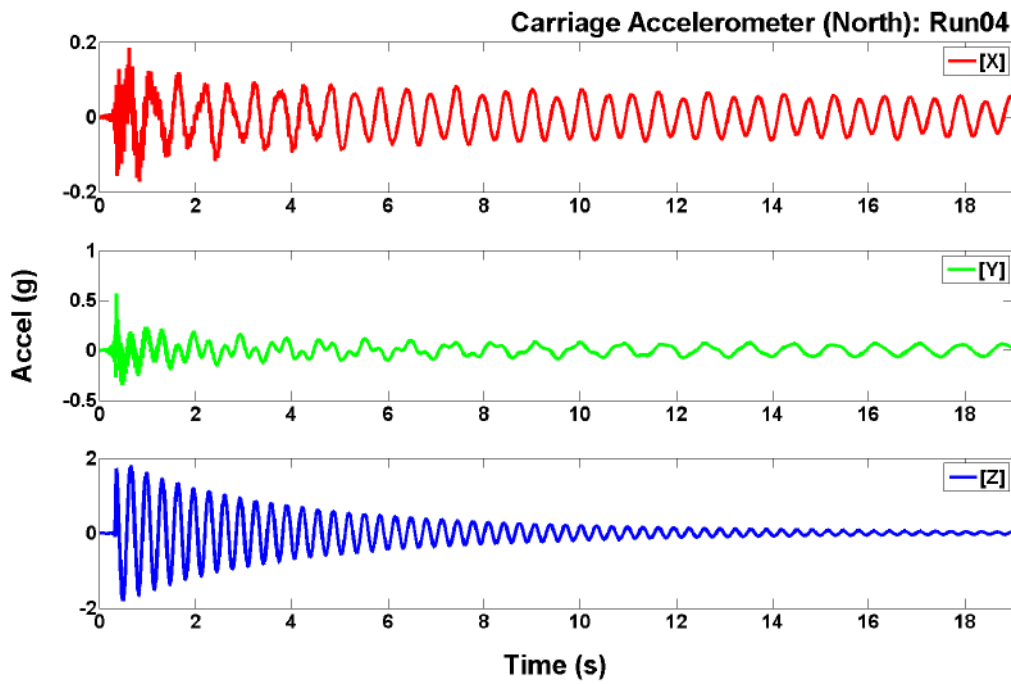


Figure 10: Raw data from top carriage accelerometer (North): Run04

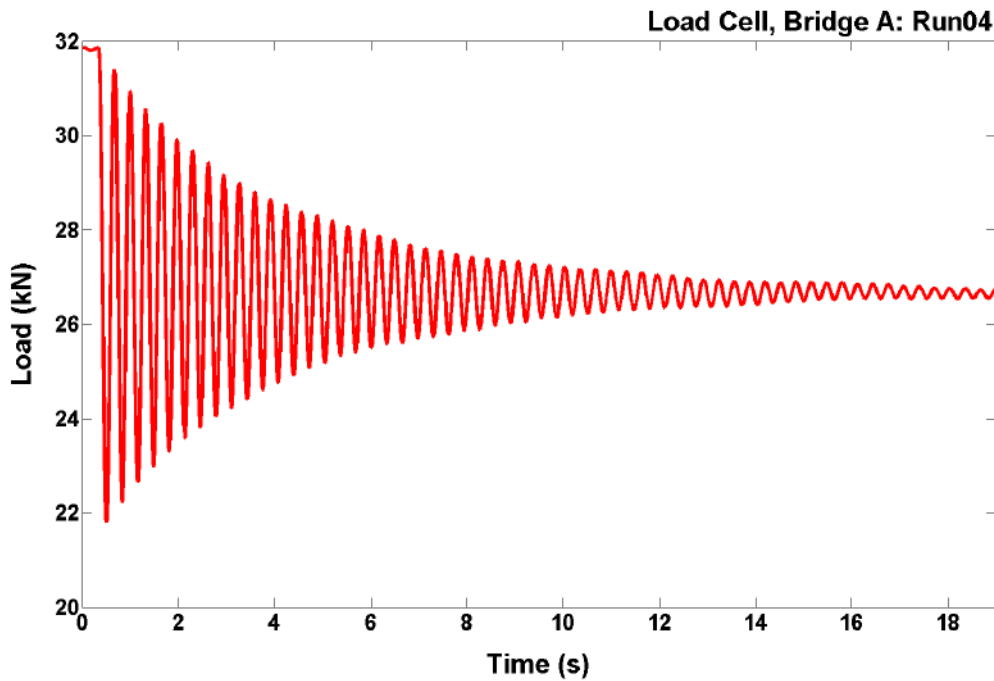


Figure 11: Raw data from load cell, Bridge A: Run04

Table 4: Damped frequency values calculated from the average between accelerometer data (carriage accelerometer – North) and load cell data (bridge A)

Run	ω_d (Hz)	ω_d (rad/s)
01	6.02	37.8
02	3.93	24.7
03	3.94	24.8
04	3.11	19.5
05	3.12	19.6
06	2.72	17.1
07	2.75	17.3
08	6.08	38.2
09	6.11	38.4

The logarithmic decrement (δ) for the load displacement was calculated from both the accelerometer and motion analysis results, and from these values the damping ratio (ζ) was calculated. The damped natural frequency (ω_d) and undamped natural frequencies (ω_n) were also calculated. Results from the accelerometer data are presented in Table 5 and the motion analysis results are presented in Table 6.

4.5.1 Analysis Method

In order to calculate the logarithmic decrement, the data was processed as follows:

- Positive peak values were identified (refer to Figures 12 and 15)
- A trend line was fitted to the peaks (refer to Figures 13 and 16)
- The logarithmic decrement was calculated between peaks from values derived from the trend line, and averaged to provide the results in Tables 5 and 6.

4.5.2 Accelerometer Data

In order to estimate the damping ratio of the load displacement, the accelerometer data was integrated twice to derive the displacement. The processing was undertaken in Matlab using a Butterworth filter with the cut-off frequency tailored to each test case. An example of the derived displacement for Run04 is presented in Figure 12 and Figure 13, with full results in Appendix C.

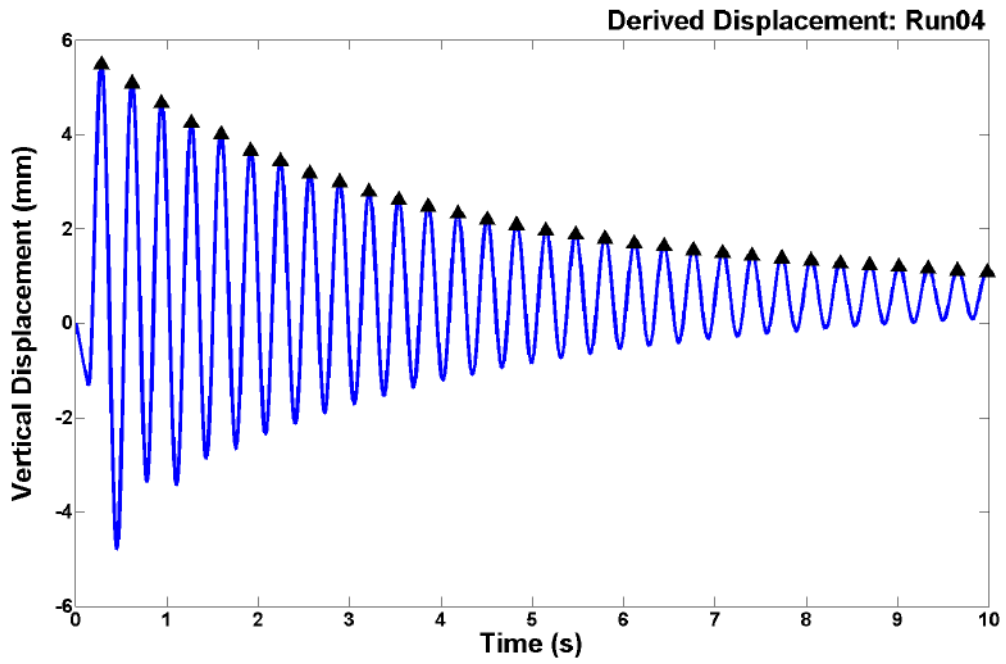


Figure 12: Peaks used for calculation of logarithmic decrement: Run04 (derived displacement)

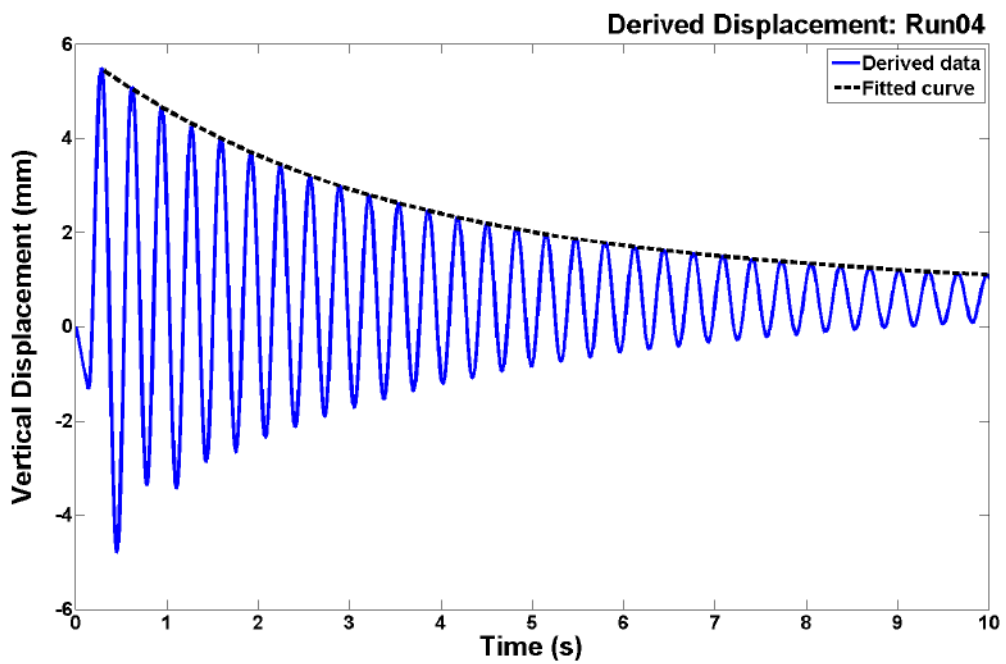


Figure 13: Trend line calculated from identified peaks: Run04 (derived displacement)

Table 5: *Logarithmic decrement, damping ratio, damped and undamped natural frequency as calculated from the accelerometer data*

Run	Logarithmic Decrement (δ)	Damping Ratio (ζ)	Damped Natural Frequency (ω_d)	Undamped Natural Frequency (ω_n)
01	0.19	0.031	6.02	6.02
02	0.11	0.018	3.93	3.93
03	0.10	0.017	3.94	3.94
04	0.06	0.008	3.11	3.11
05	0.09	0.015	3.12	3.12
06	0.11	0.019	2.72	2.72
07	0.08	0.012	2.75	2.75
08	0.09	0.010	6.08	6.08
09	0.17	0.032	6.11	6.11

When considering the derived value for undamped natural frequency (ω_n), which is calculated from the damped natural frequency (ω_d) and damping ratio (ζ) as per equation (4), it can be seen that the values are coincident. This is a reflection of the magnitude of the damping ratio which indicates that the damped natural frequency is extremely similar to the undamped natural frequency.

4.5.3 Motion Analysis Data

Shown in *Figure 14* is an example of the vertical and horizontal displacement calculated from the motion analysis data. The vertical displacement shows similar trends to the data captured from the accelerometers, which is to be expected. The horizontal displacement shows evidence of the “swing” which was induced by the load release, and is indicative of the magnitude of the out-of-plane motion. When the load was relatively light (Run01/08/09) the magnitude of the out-of-plane response increased, which increased the asymmetry in the vertical displacement.

Presented in Appendix D are the vertical and horizontal displacements calculated from the motion analysis data, including identification of the peak values used to derive the logarithmic decrement.

Unfortunately an equipment malfunction meant that Run03 was not captured by the camera equipment, and as such the result is omitted from the motion analysis.

Table 6 Logarithmic decrement, damping ratio, damped and undamped natural frequency as calculated for the motion analysis data

Run	Logarithmic Decrement (δ)	Damping Ratio (ζ)	Damped Natural Frequency (ω_d)	Undamped Natural Frequency (ω_n)
01	0.344	0.0547	6.02	6.02
02	0.214	0.0340	3.87	3.87
03	-	-	-	-
04	0.092	0.0146	3.10	3.10
05	0.084	0.0134	3.11	3.11
06	0.069	0.0110	2.70	2.70
07	0.071	0.0113	2.75	2.75
08	0.227	0.0361	5.84	5.84
09	0.203	0.0323	5.84	5.84

As previously, the undamped natural frequency calculated as per equation (4) yields the same value as the damped natural frequency, which is again a reflection of the small magnitude of the damping ratio.

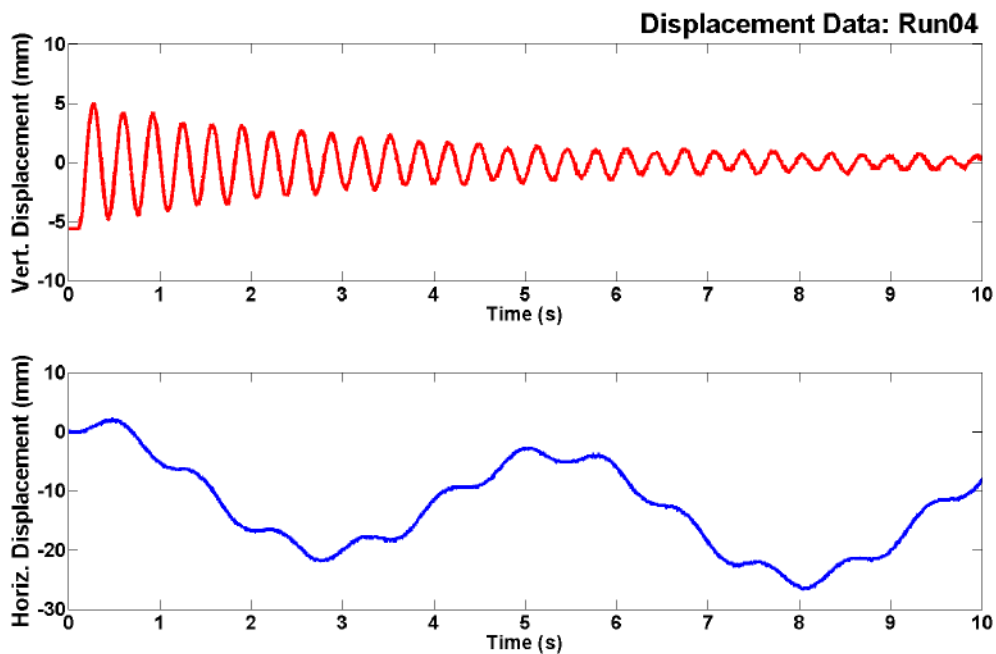


Figure 14: Vertical (top) and horizontal (lower) load displacement as calculated from motion analysis data

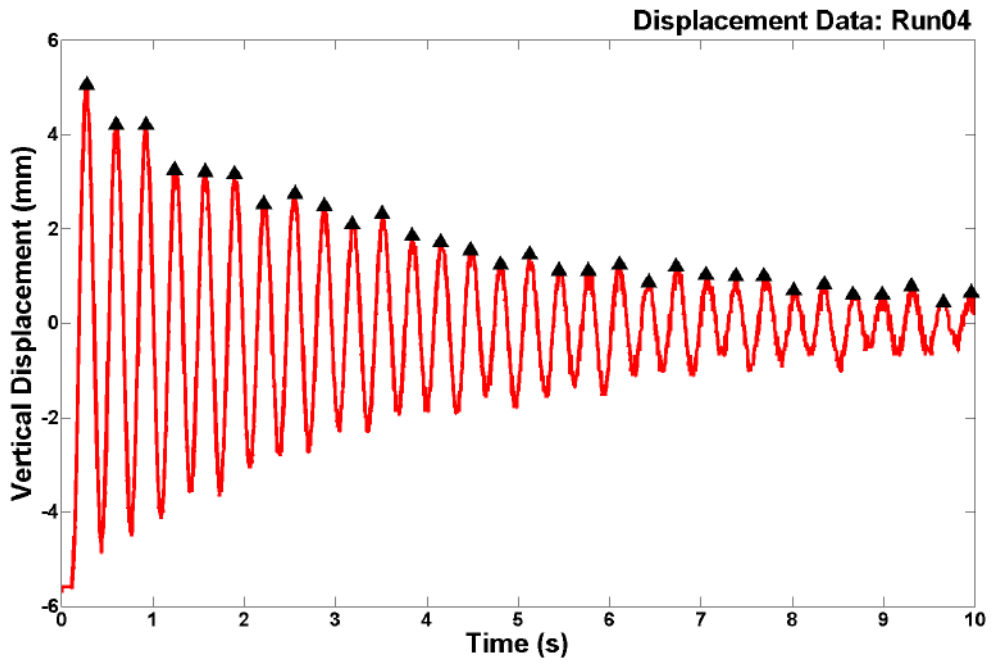


Figure 15: Peaks used for calculation of logarithmic decrement: Run04 (motion analysis data)

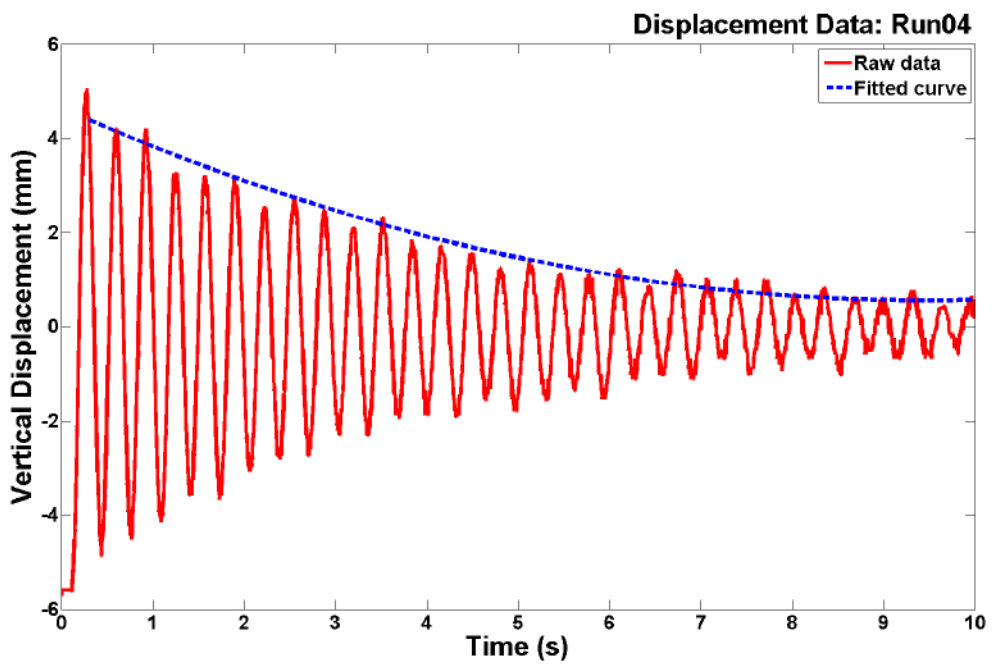


Figure 16: Trend line calculated from identified peaks: Run04 (motion analysis data)

5. Discussion

Both static and dynamic testing was undertaken on single legs of an expired HUSLE assembly in order to identify key material parameters that can be used to inform further development of simulation tools. The sling leg master lock failed at 164 kN with a maximum elongation of 228 mm under static tensile testing.

Dynamic testing across four suspended load weights yielded information relating to the damping properties of the system. Each test point was repeated to confirm the validity of the recorded results. There was very good agreement between the data collected at test points with the same suspended load. Given the small magnitude of the calculated damping ratio, the derived undamped natural frequency was coincident with the damped natural frequency.

Taking into account the nature of the roundsling material (polyester), a non-linear response under load was expected. The dynamic stiffness is reported by Latham et al. [1], which showed clear non-linear trends. As such, it was expected that the damping ratio and natural frequency of the system would vary under varying load, and this was borne out in the dynamic testing results.

Small differences can be seen between the results calculated from the accelerometer data and that derived from the motion analysis data. Given the inherent difficulty in accounting for the out-of-plane motion using the motion analysis data, the accelerometer data is considered the most appropriate data set for implementation within a simulation context.

6. Limitations and Caveats

The HUSLE assembly used for dynamic testing was expired equipment and not considered serviceable. Although the results presented here are fit for purpose with regard to improving the fidelity of simulation tools, these results **cannot** be interpreted as suitable for application in an operational context.

It should be noted that the damping parameters identified by controlled laboratory testing of a single roundsling provide the basic data required for simulation. These results cannot be considered representative of the full system under operational load. The dynamic performance of the HUSLE during flight is an inherently complex system with a large number of variables. If more detailed information is required relating to the mechanical performance of the HUSLE, further testing will be necessary.

7. References

1. Latham, C., J. Maynard, and M. Trafford, *HUSLE - Dynamic Stiffness Tests on Roundslung Assemblies*. 2012, AmSafe Bridport.
2. Bourne, K., et al., *Preliminary Testing of Helicopter Underslung Load Equipment in Support of Simulation Model Development*. 2013, DSTO.
3. AmSafe, *User Manual BG 0266-00: Helicopter Underslung Load Equipment*. 2007, AmSafe Bridport.
4. Rao, S., *Mechanical Vibrations*. Fourth ed. 2004: Prentice Hall.

Appendix A Damped Frequency from Accelerometer and Load Cell Data

Table 7: Damped frequency values calculated from accelerometer data (carriage accelerometer – North) and load cell data (bridge A)

Run	Accelerometer Data (Hz)			Load Cell Data (Hz)		
	f_{min}	f_{max}	f_{mean}	f_{min}	f_{max}	f_{mean}
01	5.92	6.56	6.34	5.92	6.83	6.41
02	3.84	4.18	3.93	3.86	4.02	3.93
03	3.82	4.21	3.94	3.87	4.02	3.94
04	3.03	3.23	3.11	3.06	3.18	3.11
05	3.07	3.16	3.12	3.07	3.19	3.12
06	2.67	2.78	2.72	2.62	2.82	2.72
07	2.69	2.84	2.75	2.70	2.80	2.75
08	5.69	6.28	6.08	5.75	6.36	6.08
09	5.69	6.48	6.11	5.81	6.32	6.10

This page is intentionally blank.

Appendix B Load Cell and Accelerometer Data – Response Profiles

B.1 Run01: Suspended Weight 560 kg, Preload total 1050 kg

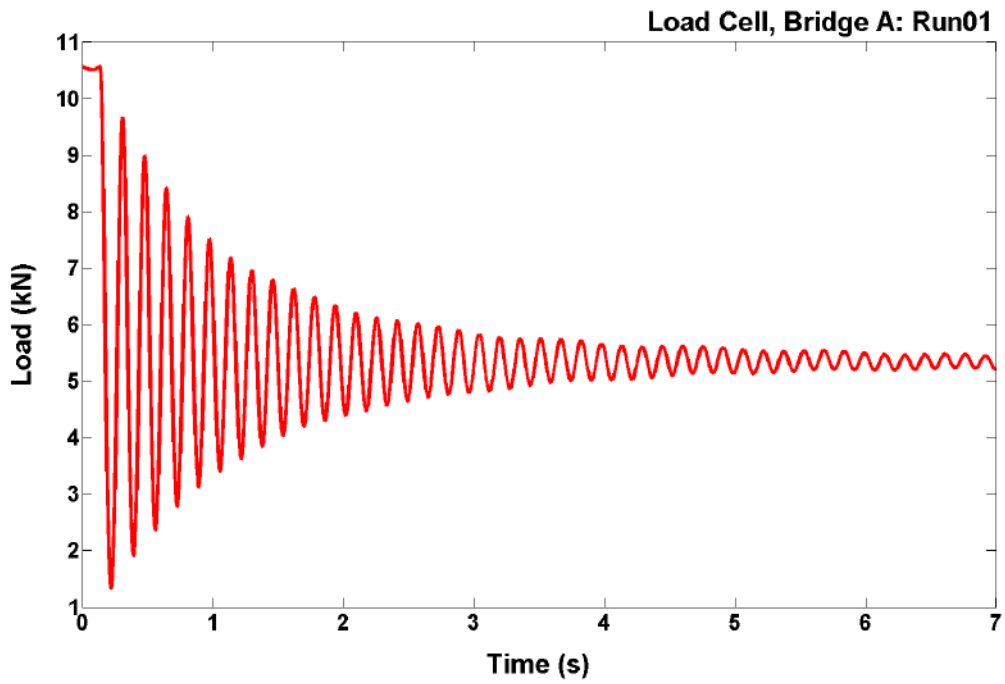


Figure 17: Raw data from load cell, Bridge A: Run01

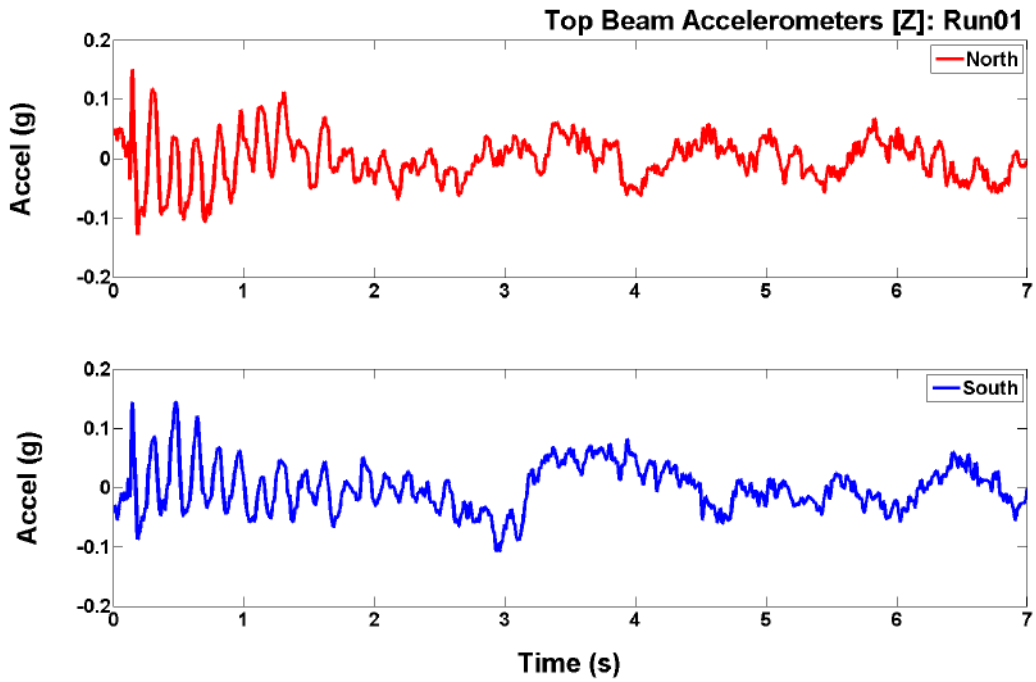


Figure 18: Raw data from top beam accelerometers: Run01

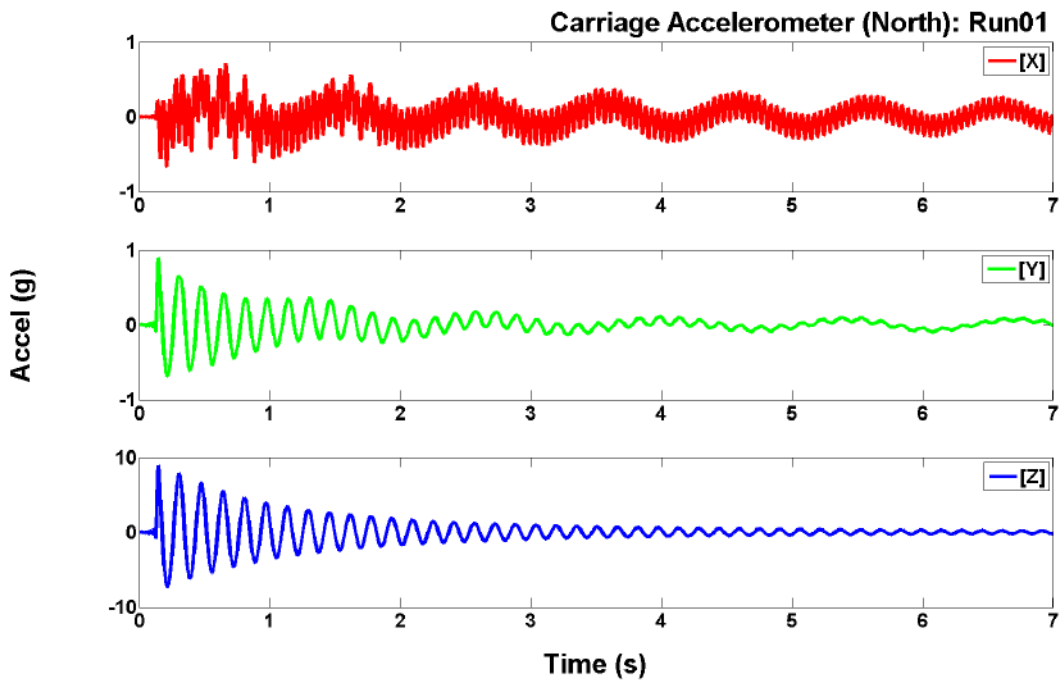


Figure 19: Raw data from top carriage accelerometer (North): Run01

B.2 Run02: Suspended weight 560 kg, Preload total 1050 kg

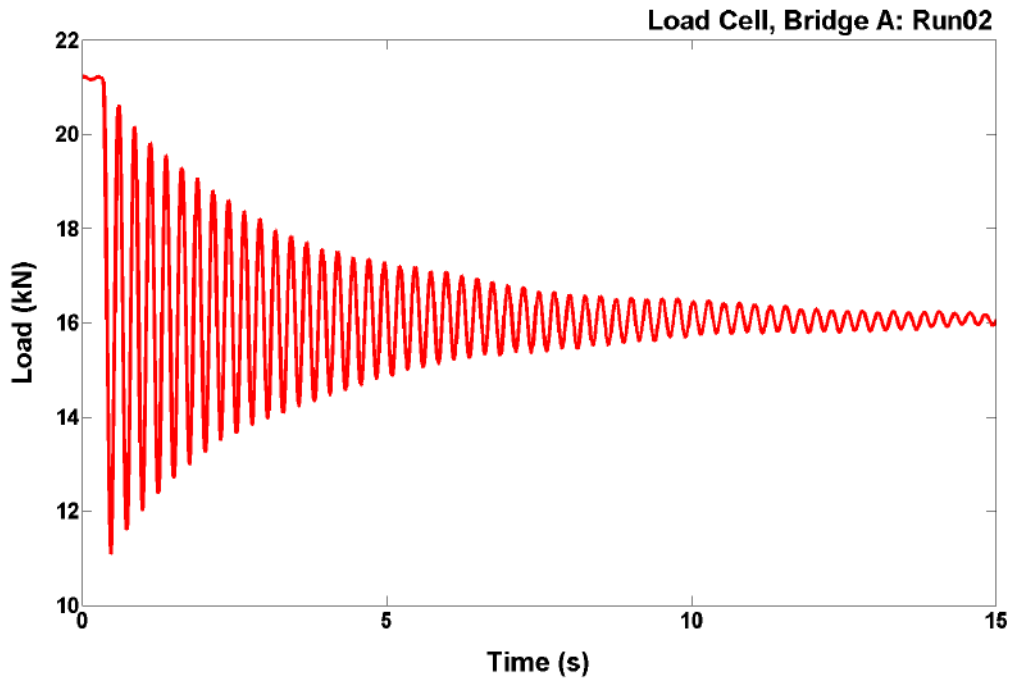


Figure 20: Raw data from load cell, Bridge A: Run02

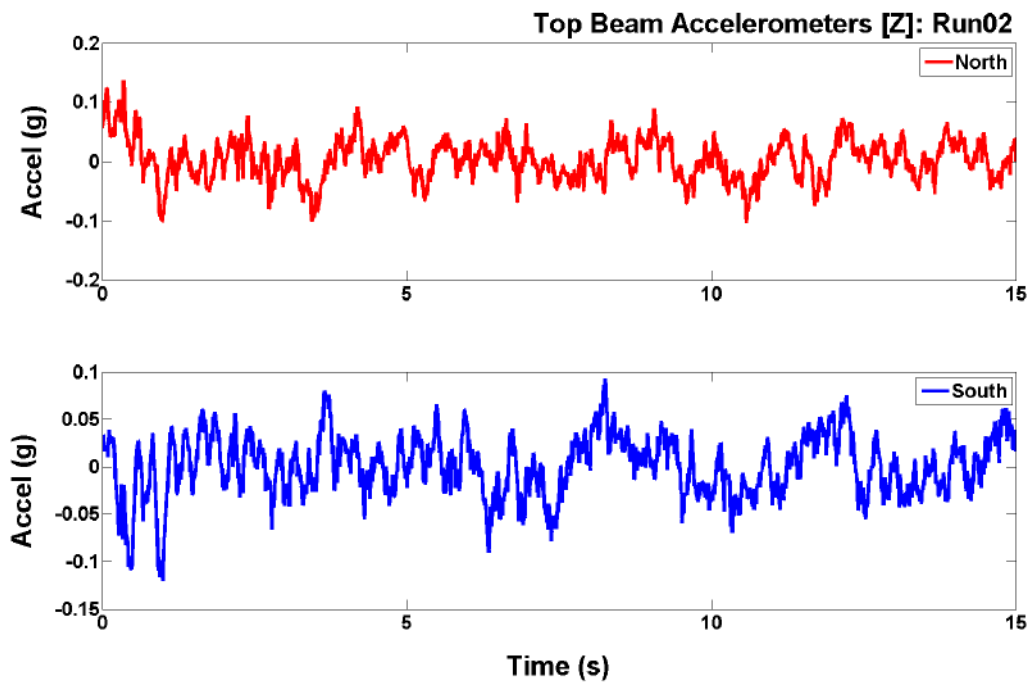


Figure 21: Raw data from top beam accelerometers: Run02

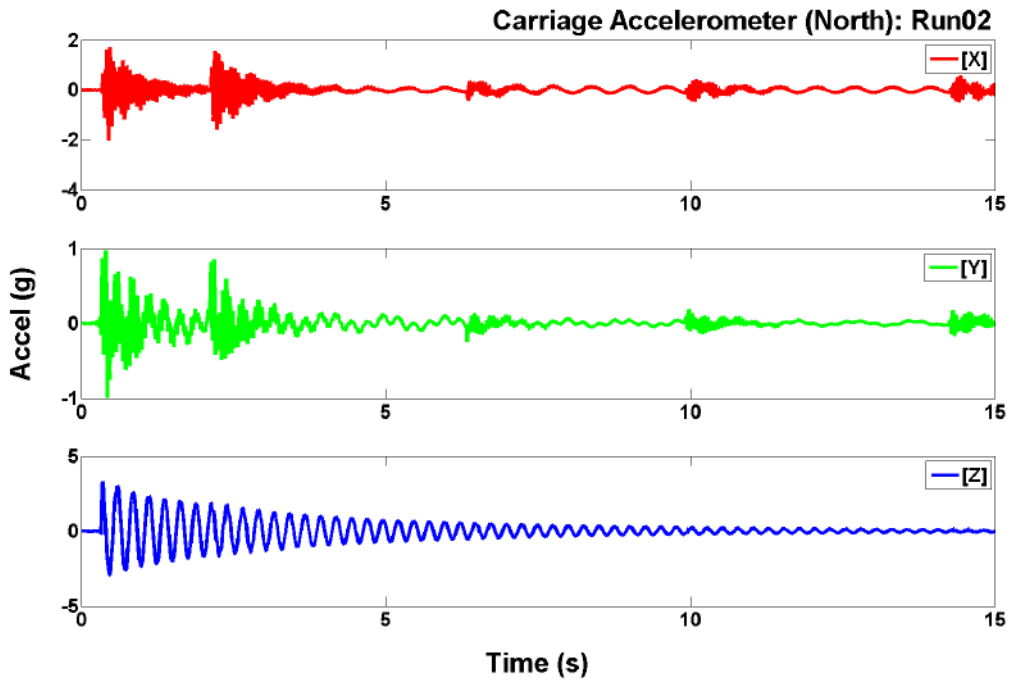


Figure 22: Raw data from top carriage accelerometer (North): Run02

B.3 Run03: Suspended weight 1615 kg, Preload total 2130 kg

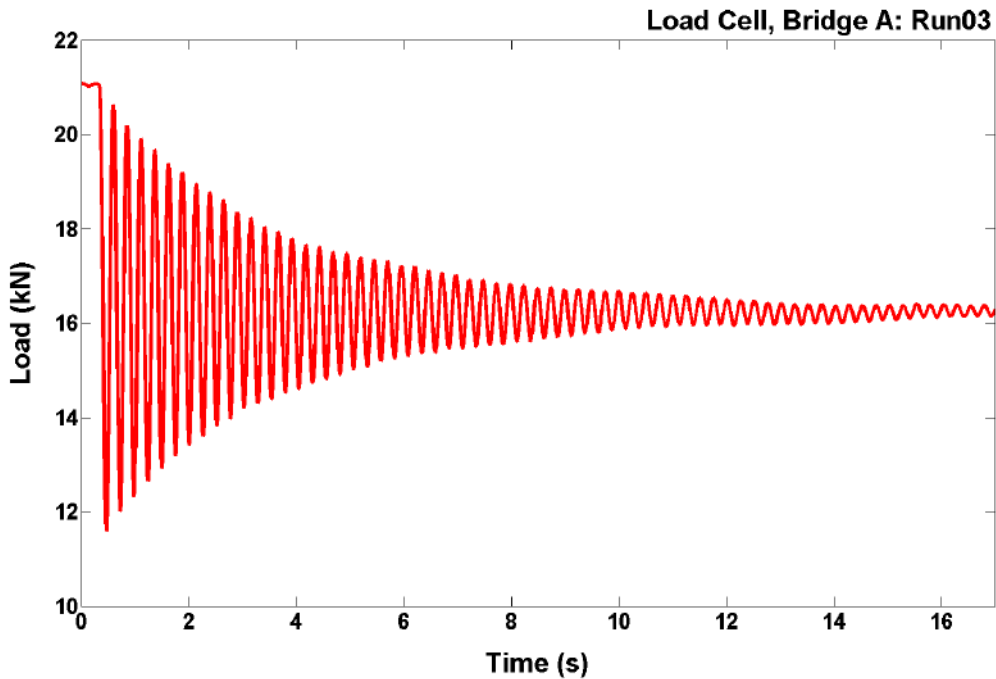


Figure 23: Raw data from load cell, Bridge A: Run03

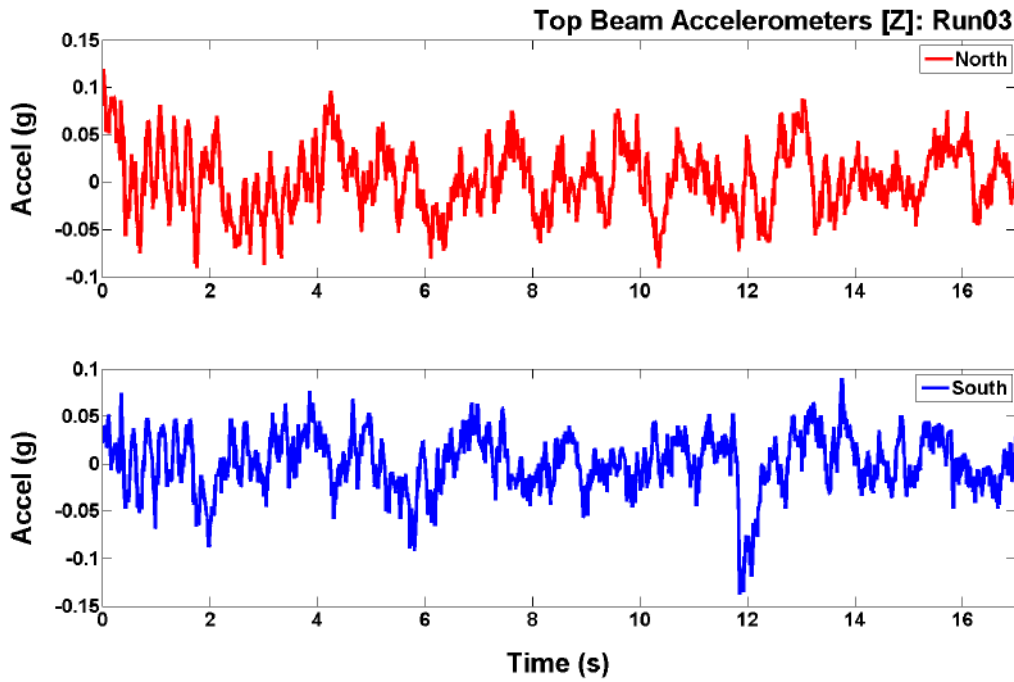


Figure 24: Raw data from top beam accelerometers: Run03

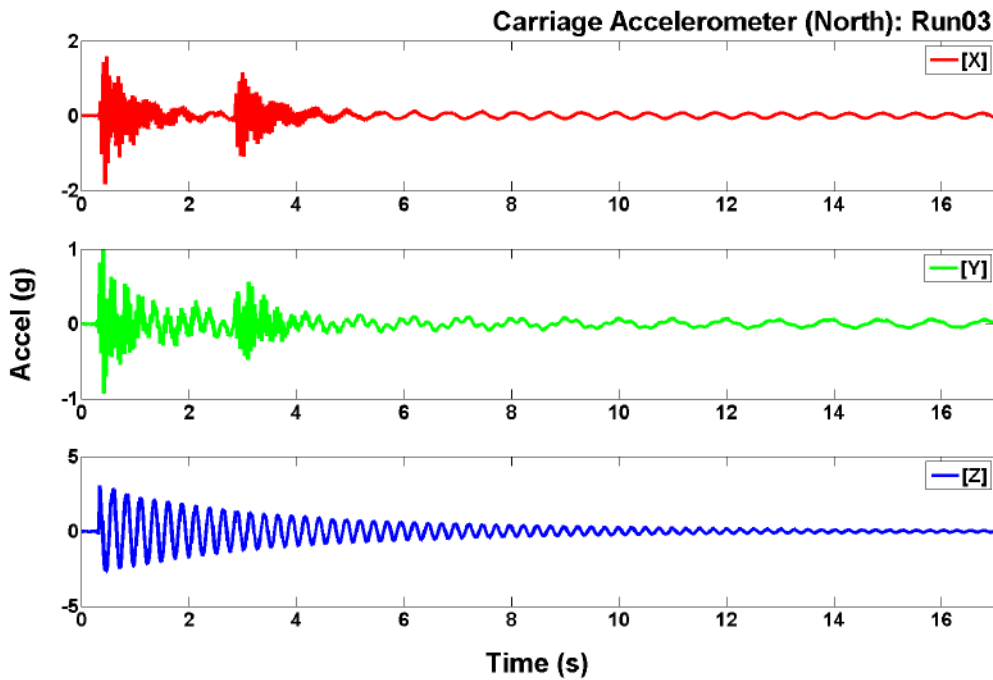


Figure 25: Raw data from top carriage accelerometer (North): Run03

B.4 Run04: Suspended weight 2670 kg, Preload total 3220 kg

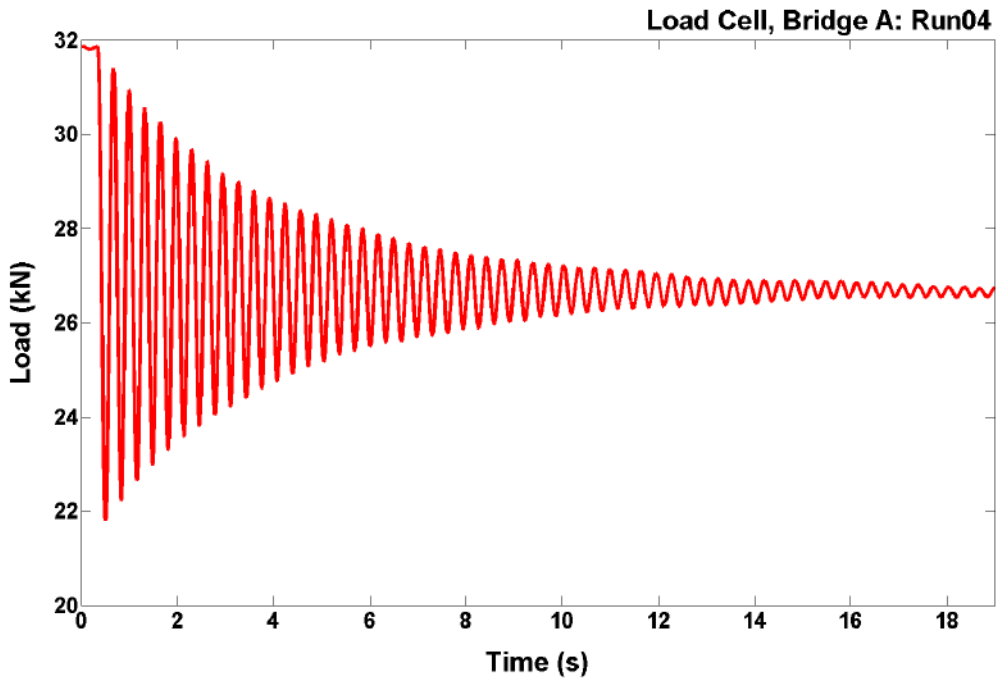


Figure 26: Raw data from load cell, Bridge A: Run04

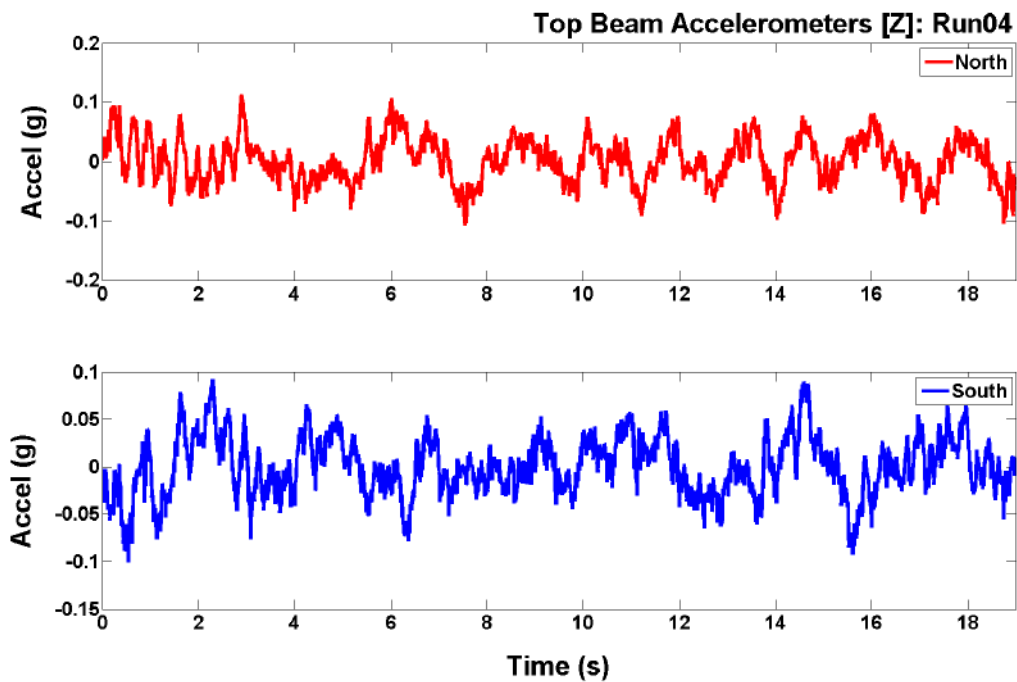


Figure 27: Raw data from top beam accelerometers: Run04

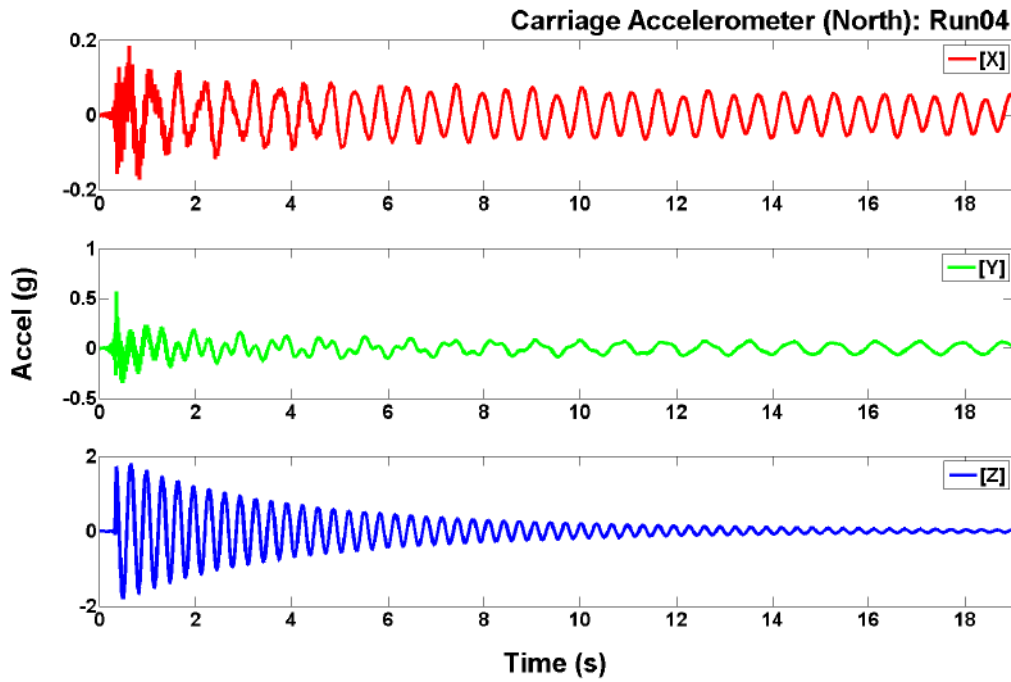


Figure 28: Raw data from top carriage accelerometer (North): Run04

B.5 Run05: Suspended weight 2685 kg, Preload total 3205 kg

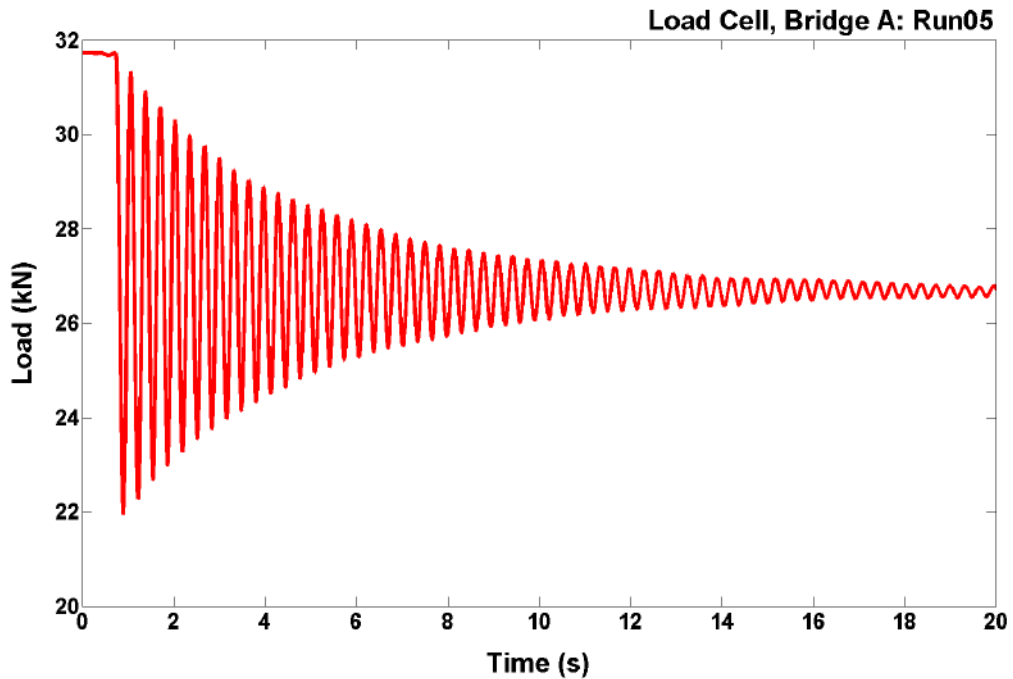


Figure 29: Raw data from load cell, Bridge A: Run05

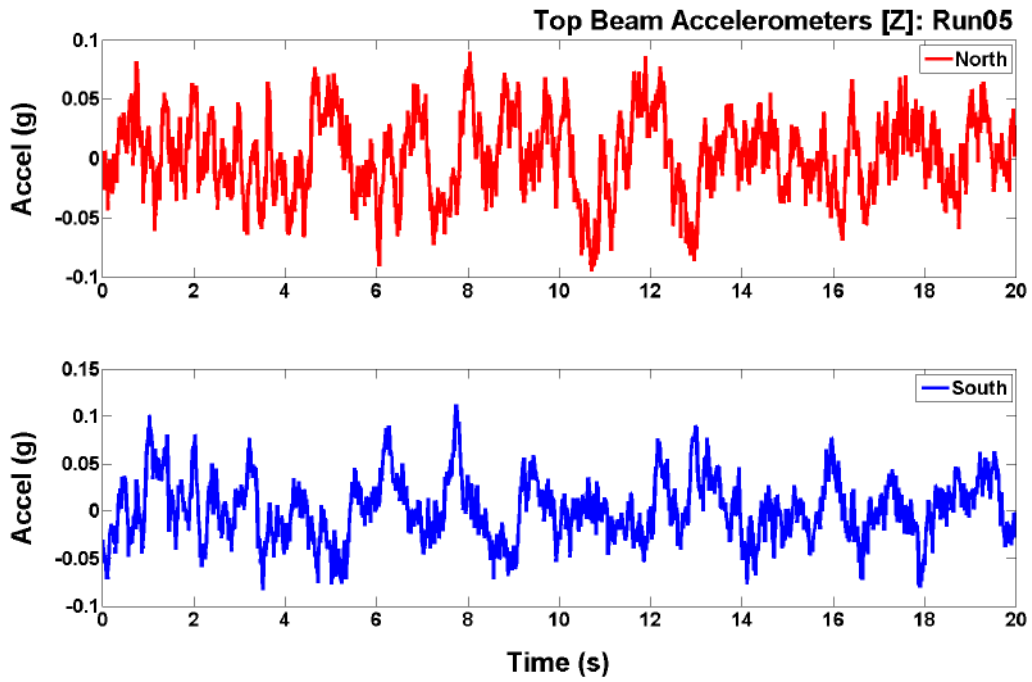


Figure 30: Raw data from top beam accelerometers: Run05

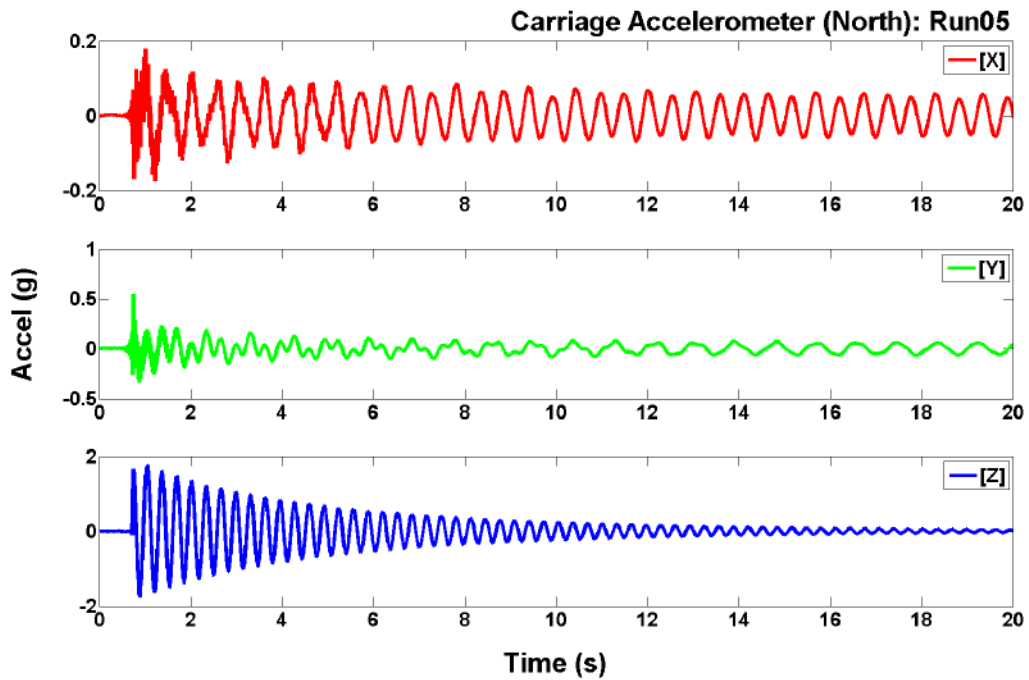


Figure 31: Raw data from top carriage accelerometer (North): Run05

B.6 Run06: Suspended weight 3763 kg, Preload total 4290 kg

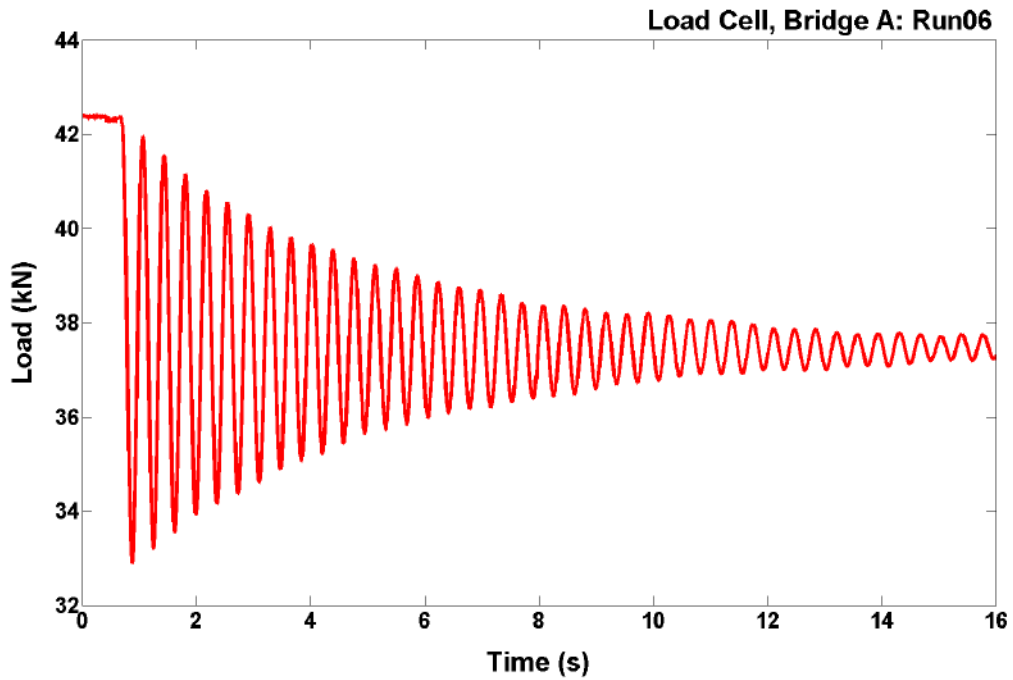


Figure 32: Raw data from load cell, Bridge A: Run06

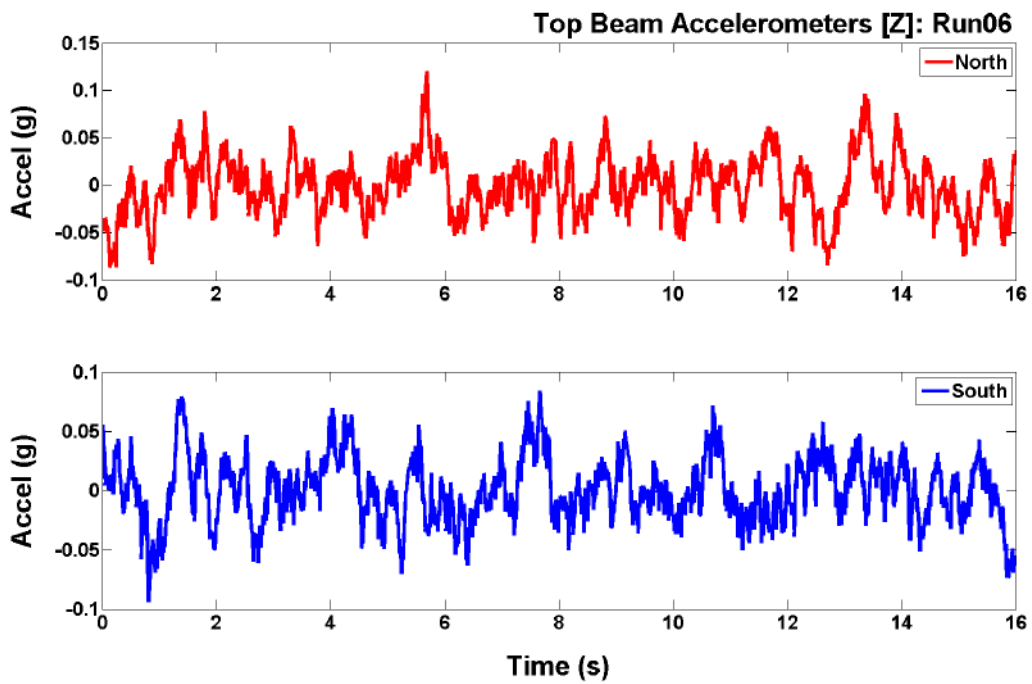


Figure 33: Raw data from top beam accelerometers: Run06

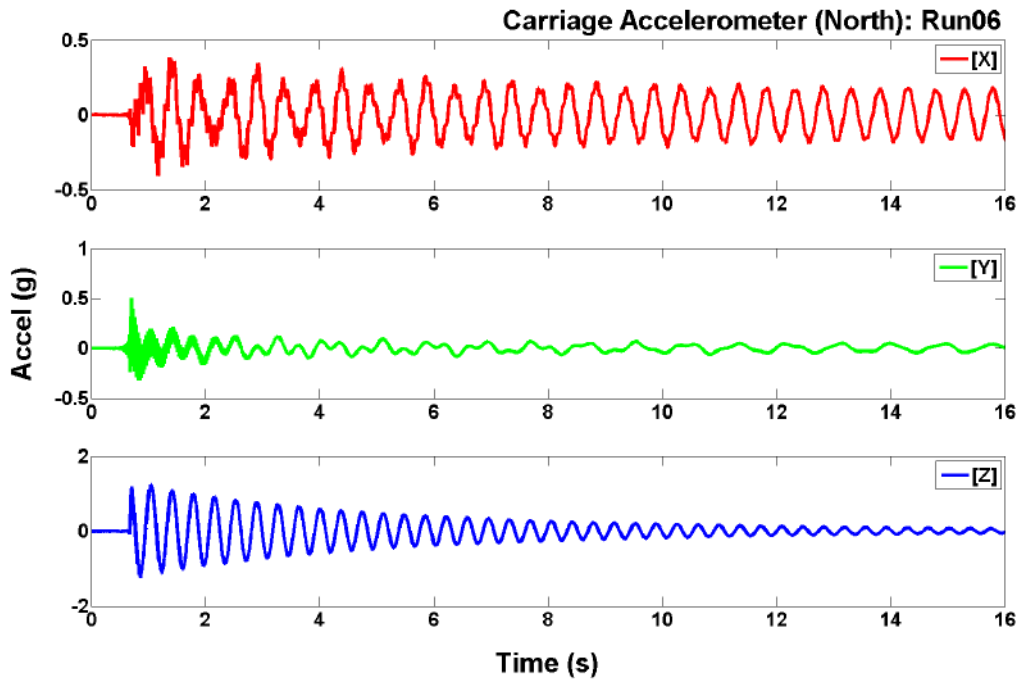


Figure 34: Raw data from top carriage accelerometer (North): Run06

B.7 Run07: Suspended weight 3770 kg, Preload total 4280 kg

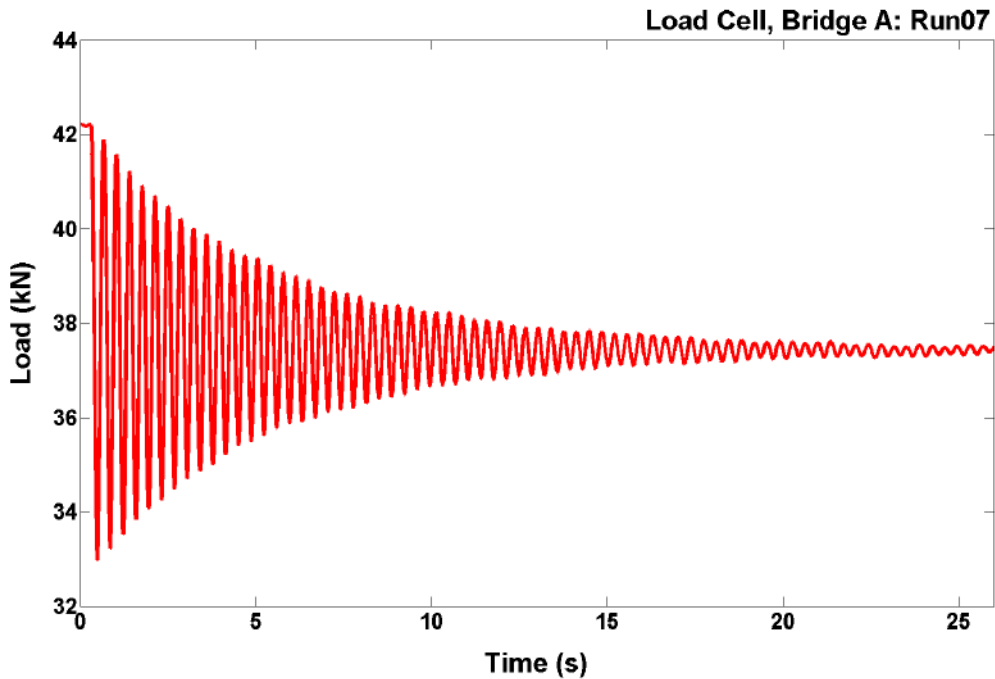


Figure 35: Raw data from load cell, Bridge A: Run07

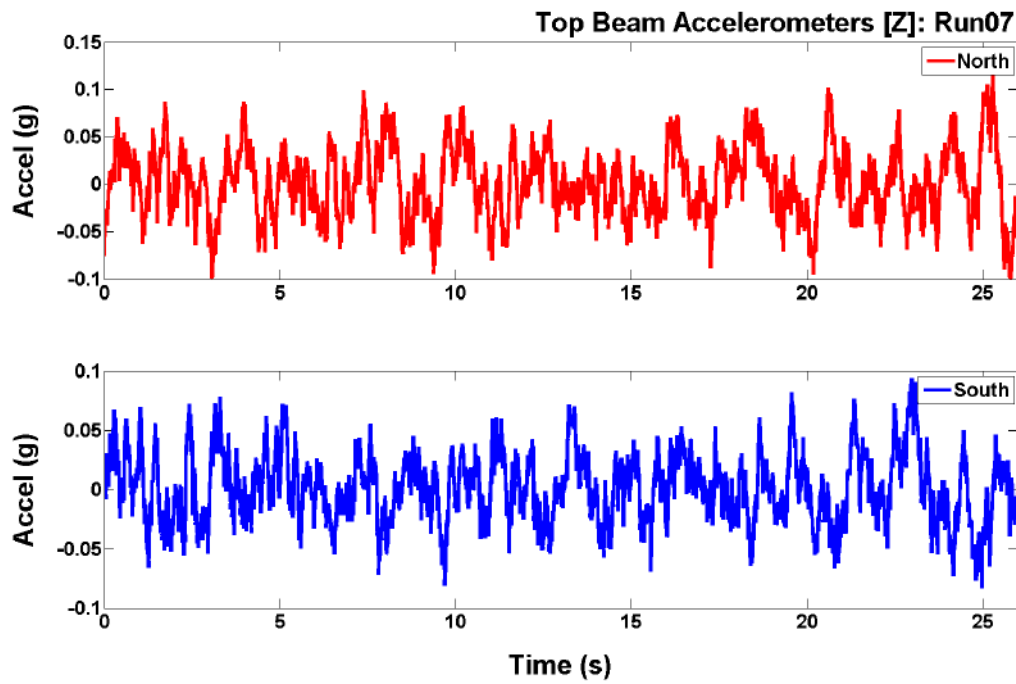


Figure 36: Raw data from top beam accelerometers: Run07

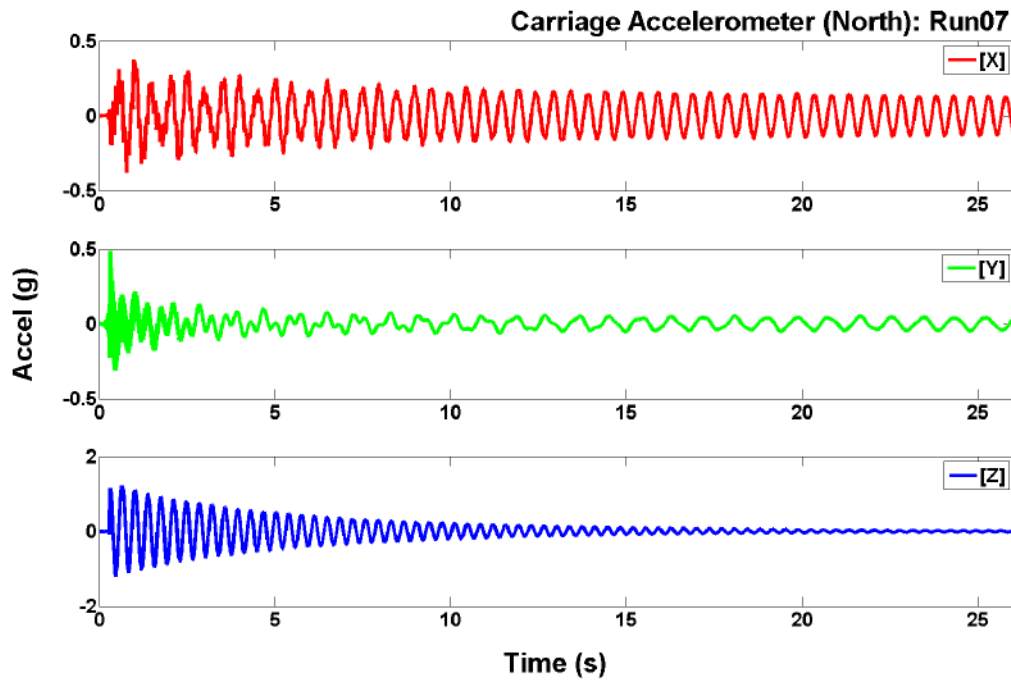


Figure 37: Raw data from top carriage accelerometer (North): Run07

B.8 Run08: Suspended weight 550 kg, Preload total 1045 kg

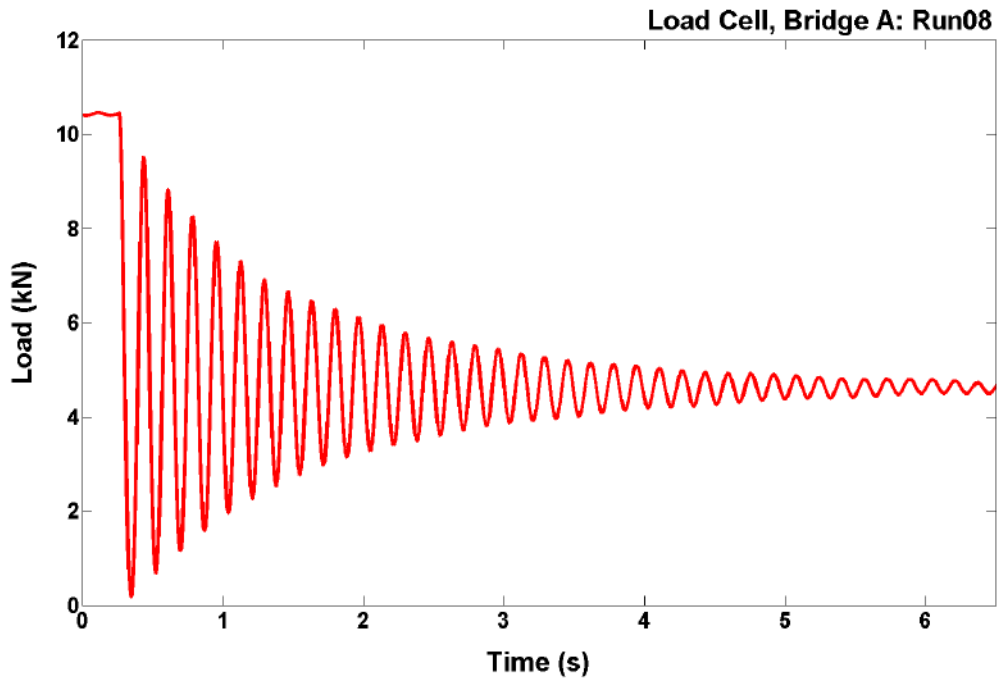


Figure 38: Raw data from load cell, Bridge A: Run08

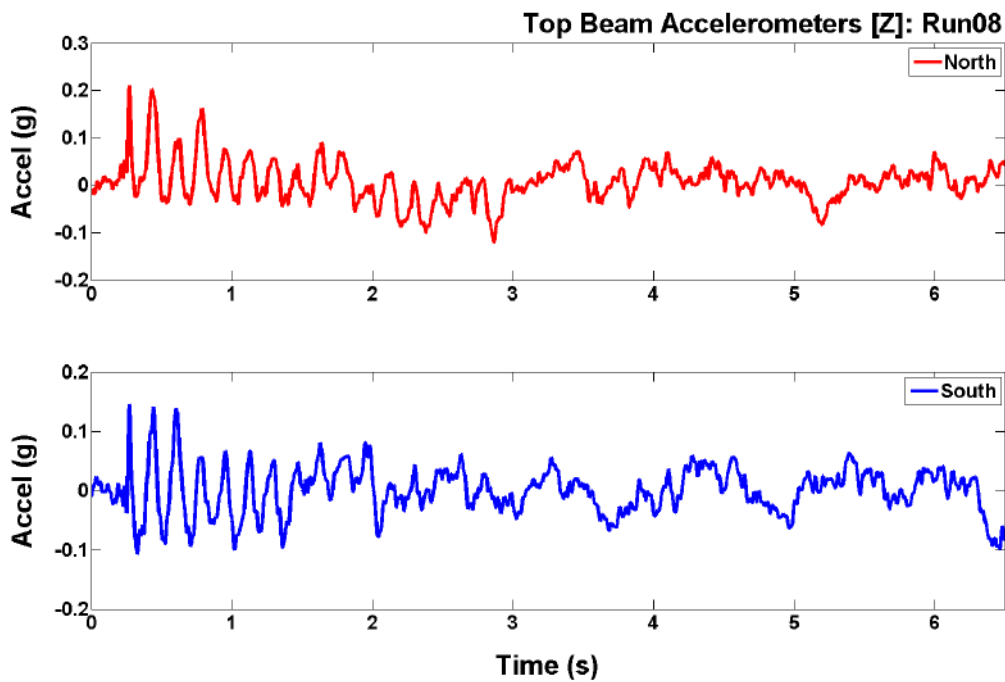


Figure 39: Raw data from top beam accelerometers: Run08

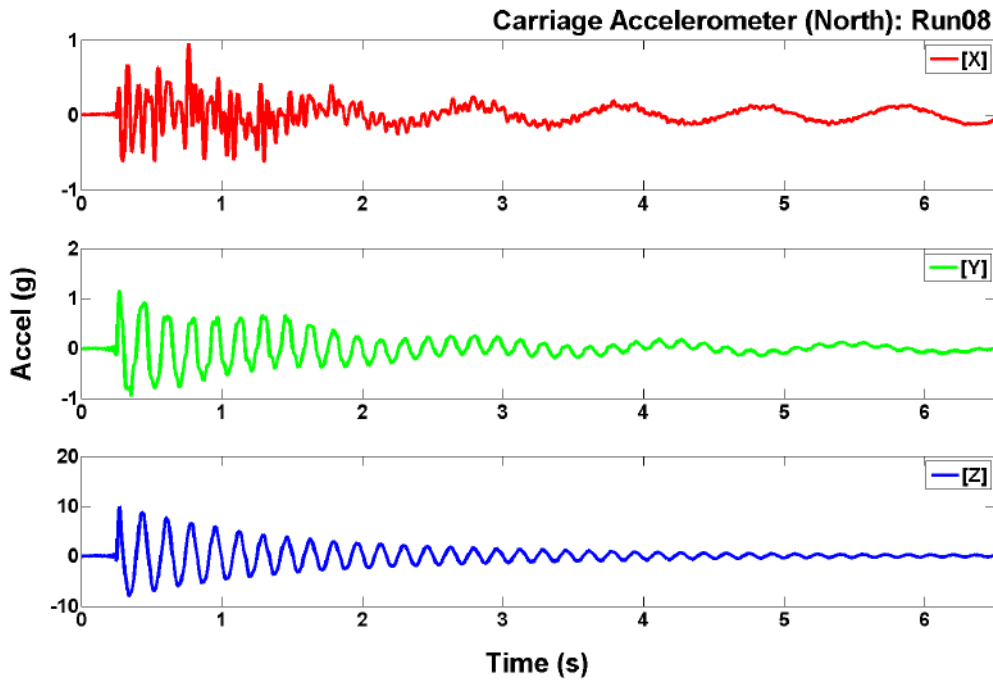


Figure 40: Raw data from top carriage accelerometer (North): Run08

B.9 Run09: Suspended weight 552 kg, Preload total 970 kg

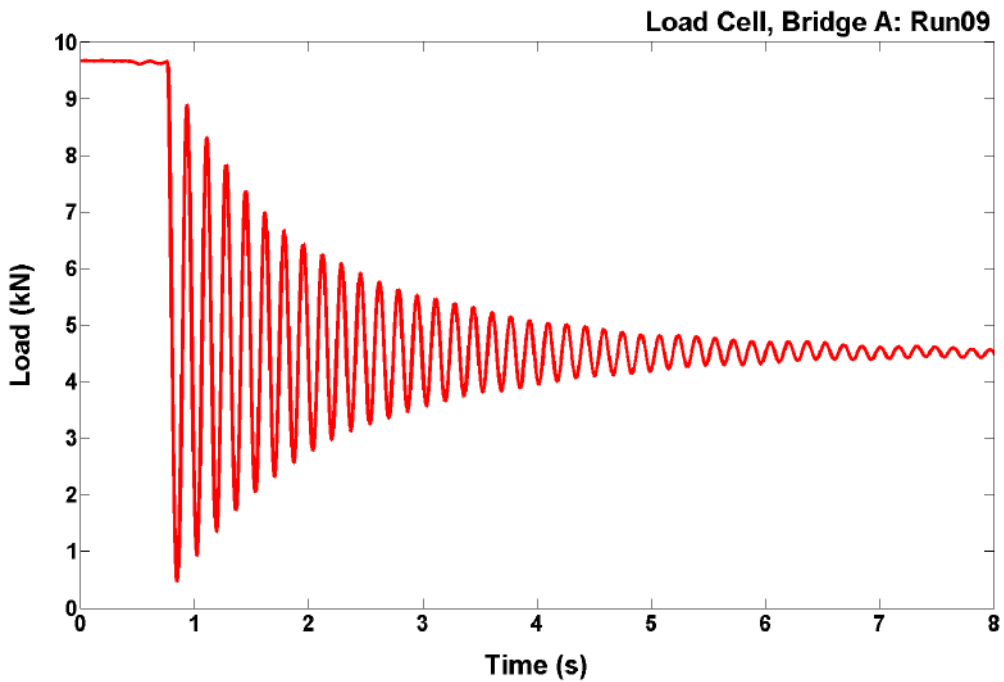


Figure 41: Raw data from load cell, Bridge A: Run09

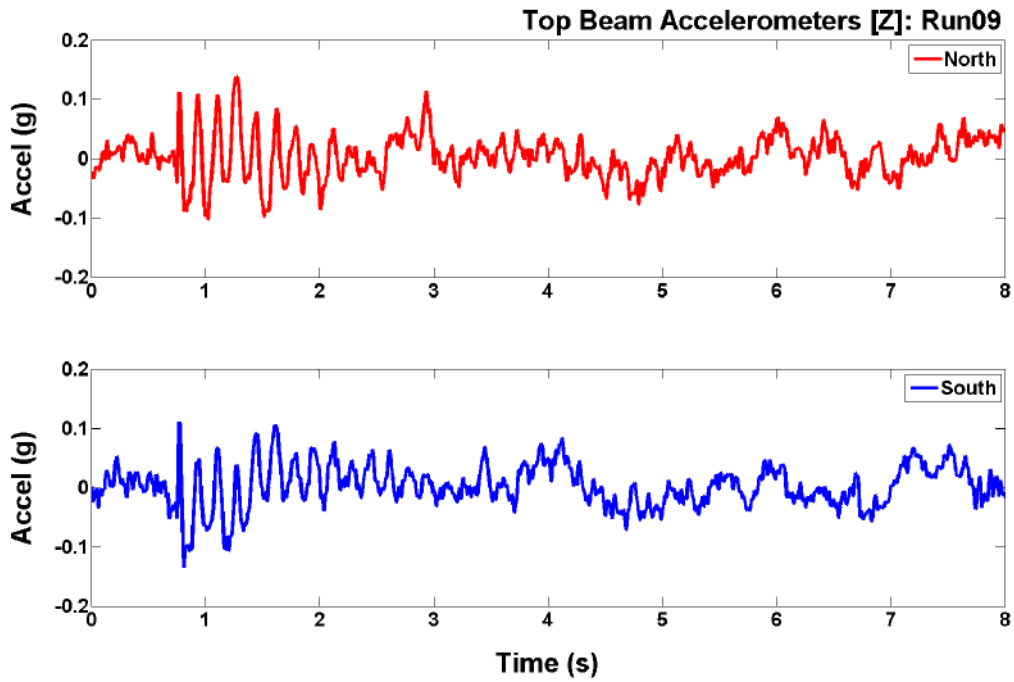


Figure 42: Raw data from top beam accelerometers: Run09

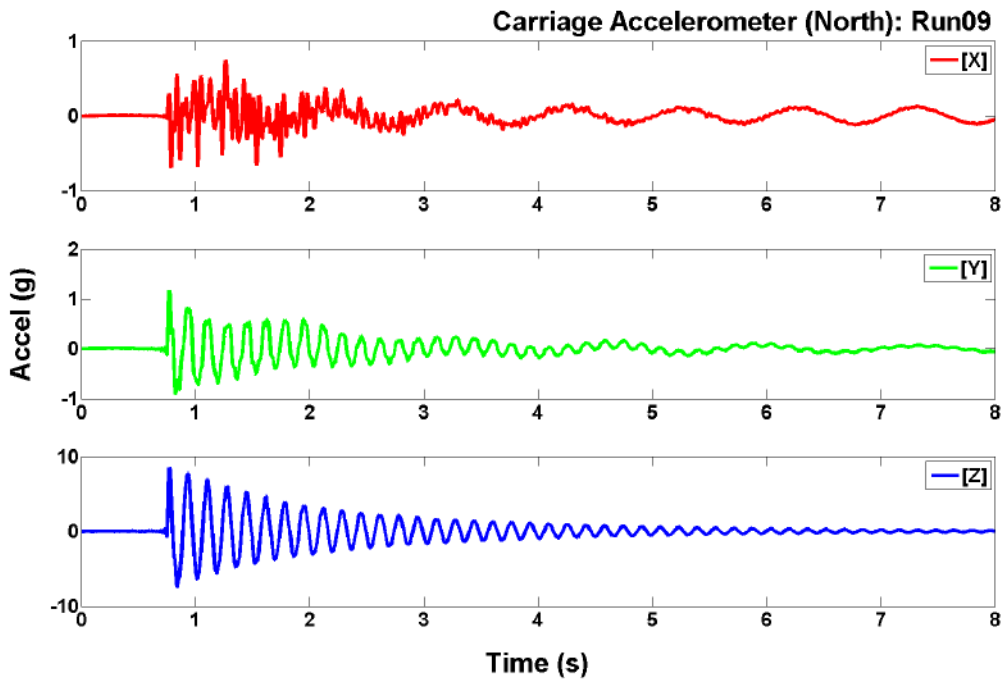


Figure 43: Raw data from top carriage accelerometer (North): Run09

Appendix C Displacement Derived from Accelerometer Data

C.1 Run01: Suspended Weight 560kg, Preload total 1050kg

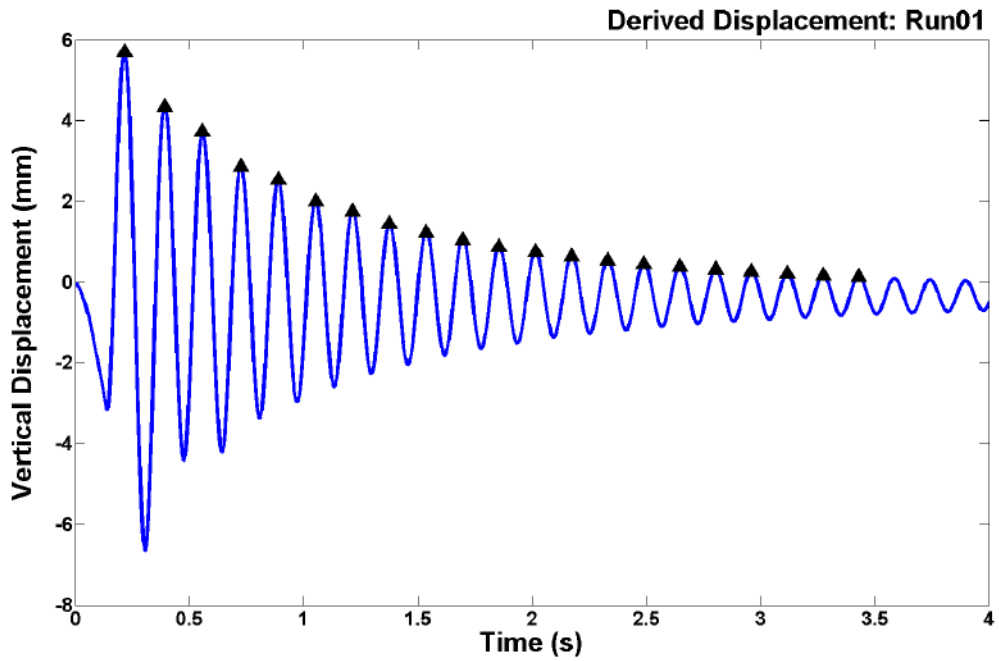


Figure 44: Peaks used for calculation of logarithmic decrement: Run01

C.2 Run02: Suspended weight 560 kg, Preload total 1050 kg

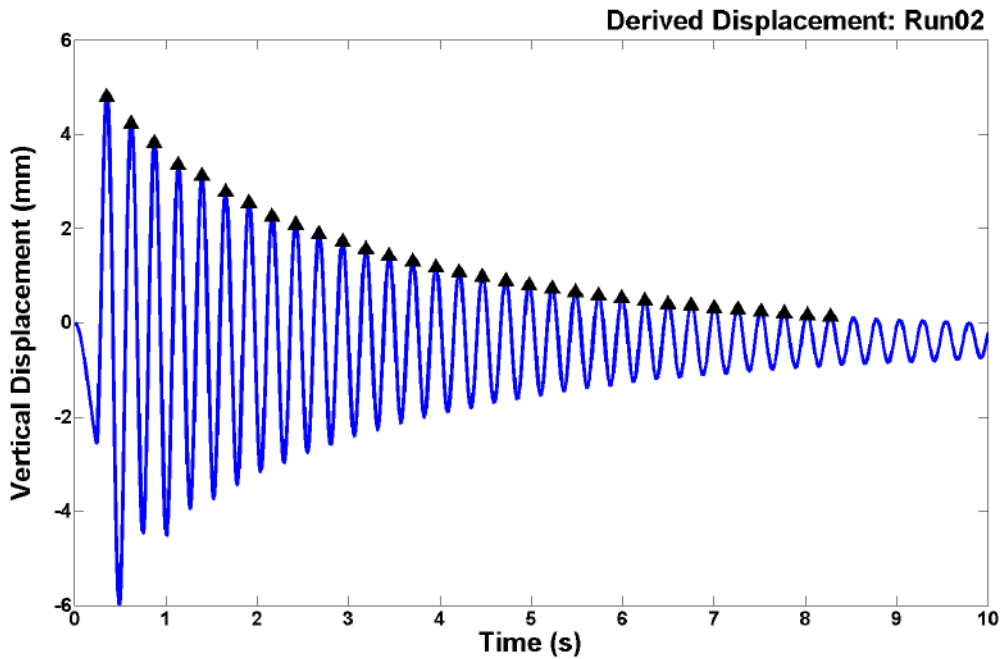


Figure 45: Peaks used for calculation of logarithmic decrement: Run02

C.3 Run03: Suspended weight 1615 kg, Preload total 2130 kg

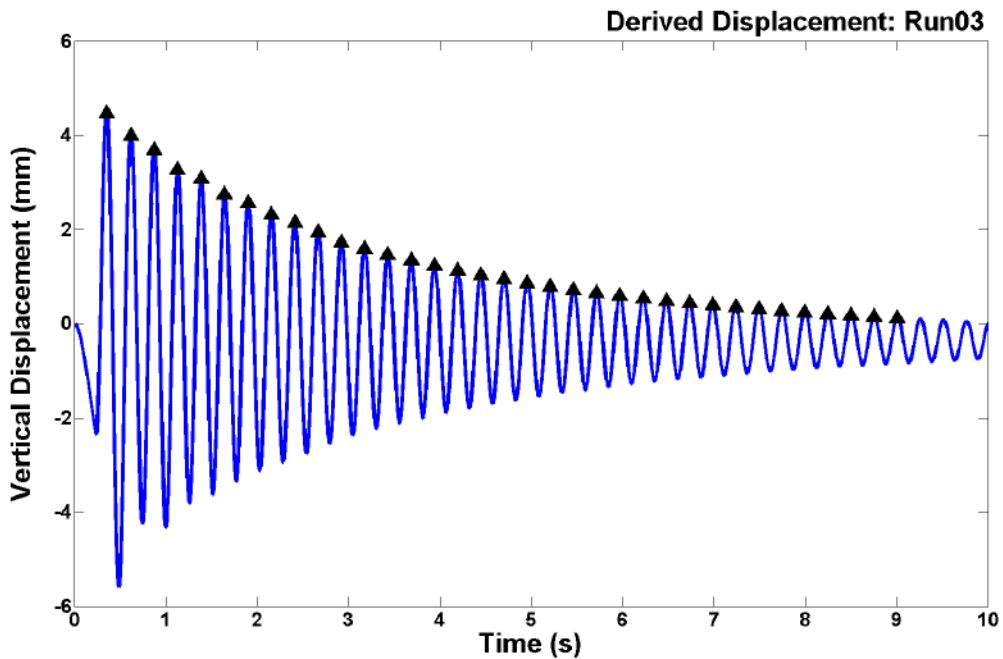


Figure 46: Peaks used for calculation of logarithmic decrement: Run03

C.4 Run04: Suspended weight 2670 kg, Preload total 3220 kg

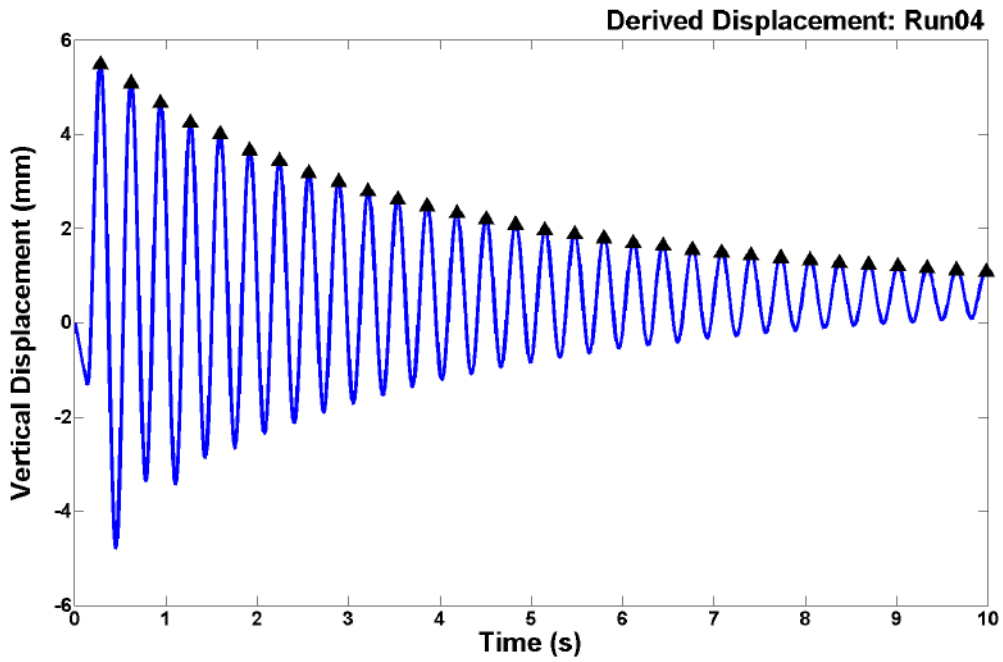


Figure 47: Peaks used for calculation of logarithmic decrement: Run04

C.5 Run05: Suspended weight 2685 kg, Preload total 3205 kg

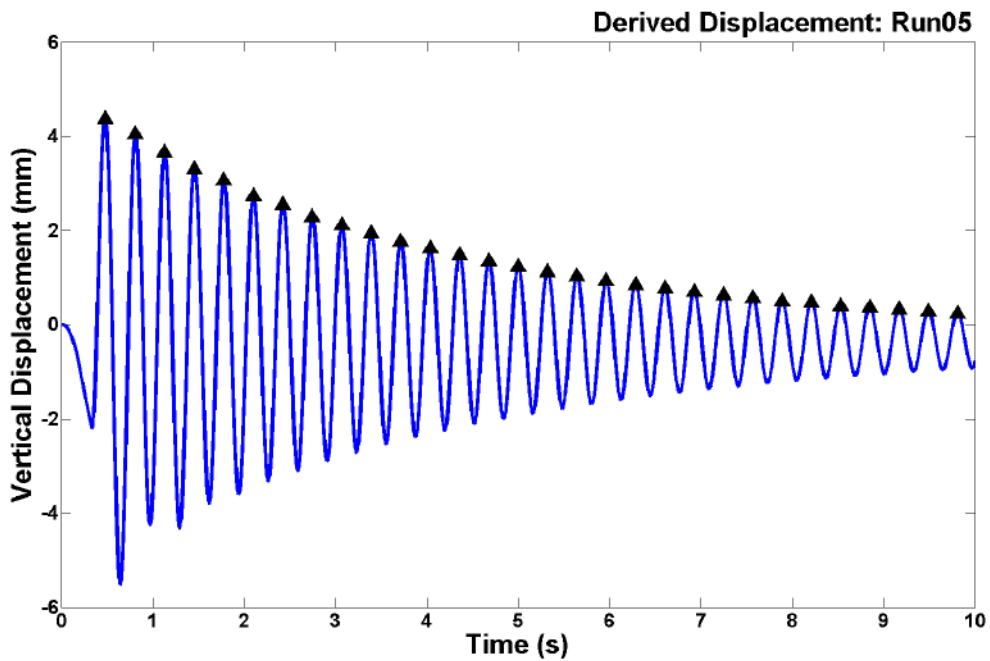


Figure 48: Peaks used for calculation of logarithmic decrement: Run05

C.6 Run06: Suspended weight 3763 kg, Preload total 4290 kg

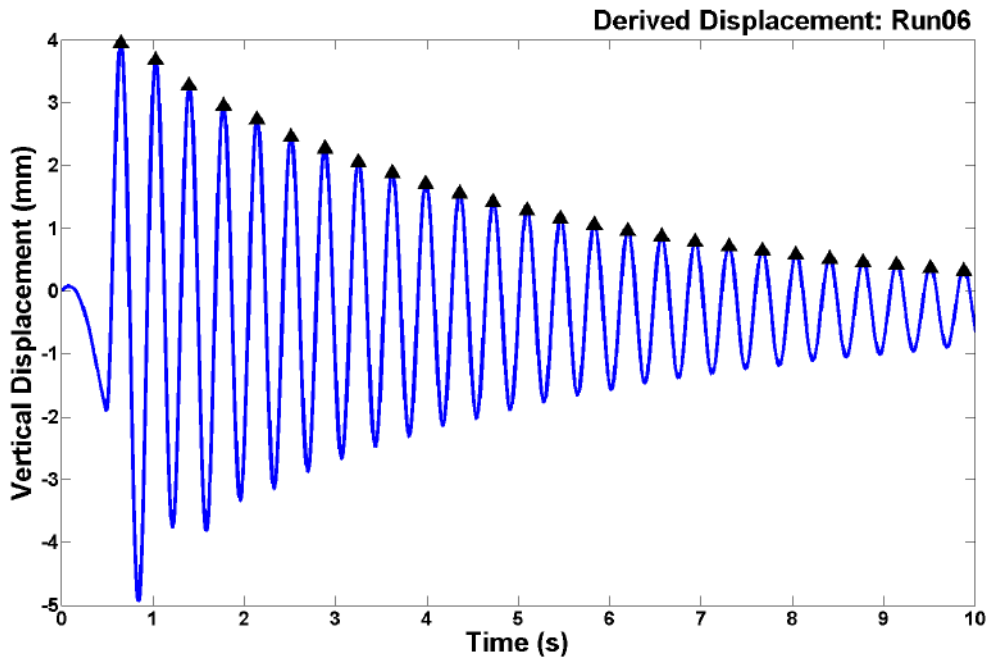


Figure 49: Peaks used for calculation of logarithmic decrement: Run06

C.7 Run07: Suspended weight 3770 kg, Preload total 4280 kg

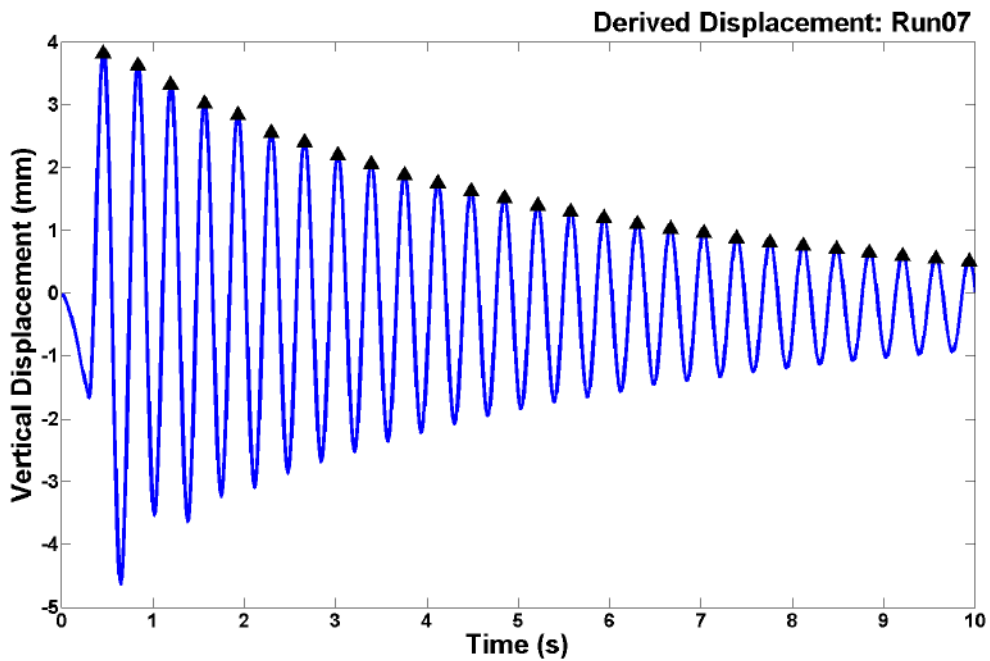


Figure 50: Peaks used for calculation of logarithmic decrement: Run07

C.8 Run08: Suspended weight 550 kg, Preload total 1045 kg

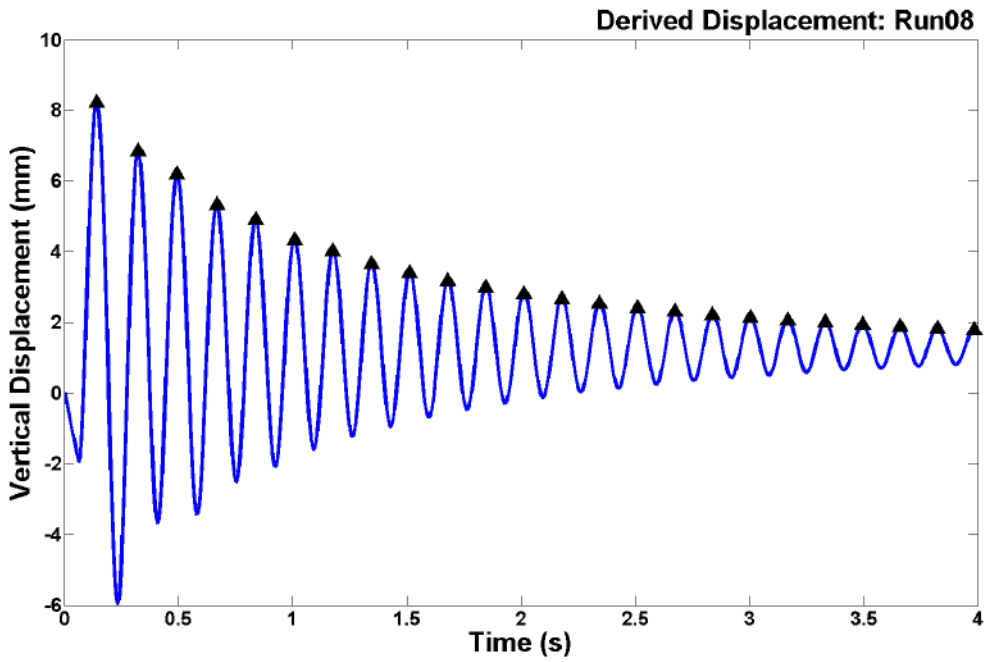


Figure 51: Peaks used for calculation of logarithmic decrement: Run08

C.9 Run09: Suspended weight 552 kg, Preload total 970 kg

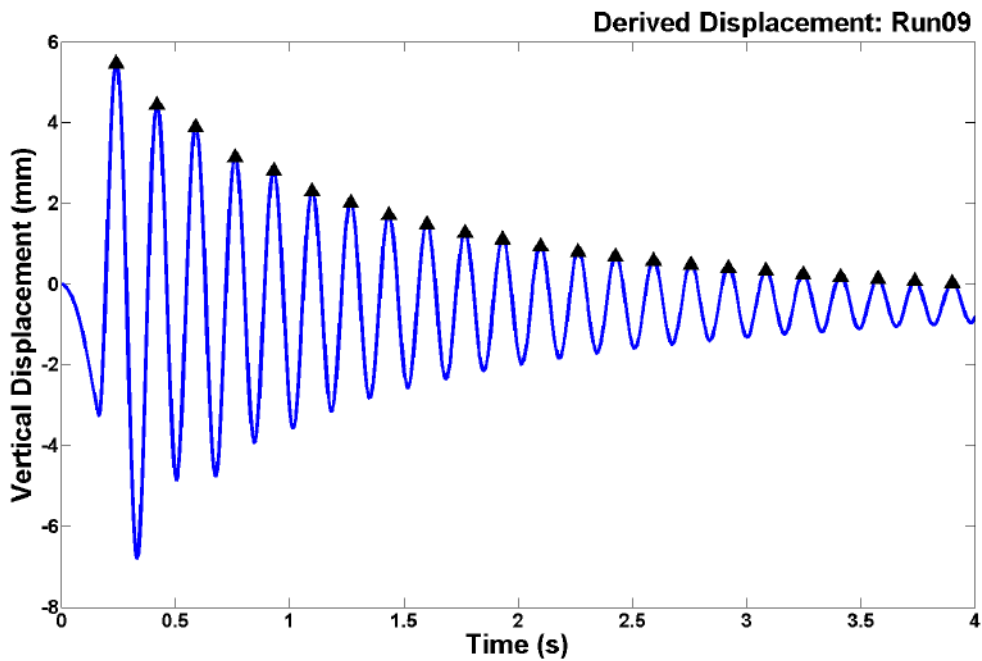


Figure 52: Peaks used for calculation of logarithmic decrement: Run09

This page is intentionally blank.

Appendix D Motion Analysis Data

D.1 Run01: Suspended Weight 560kg, Preload total 1050kg

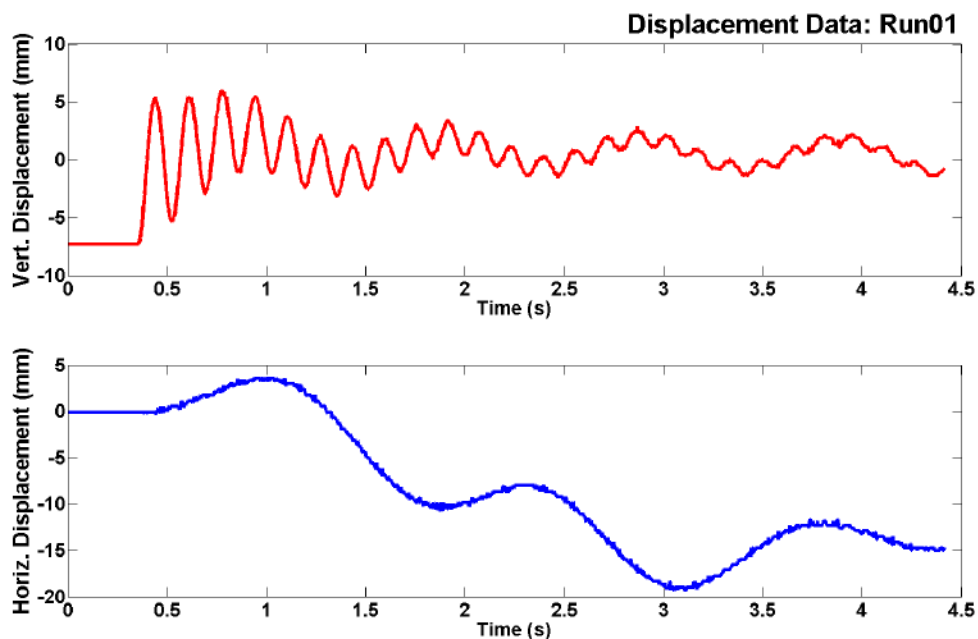


Figure 53: Vertical (top) and horizontal (lower) load displacement as calculated from motion analysis data: Run01

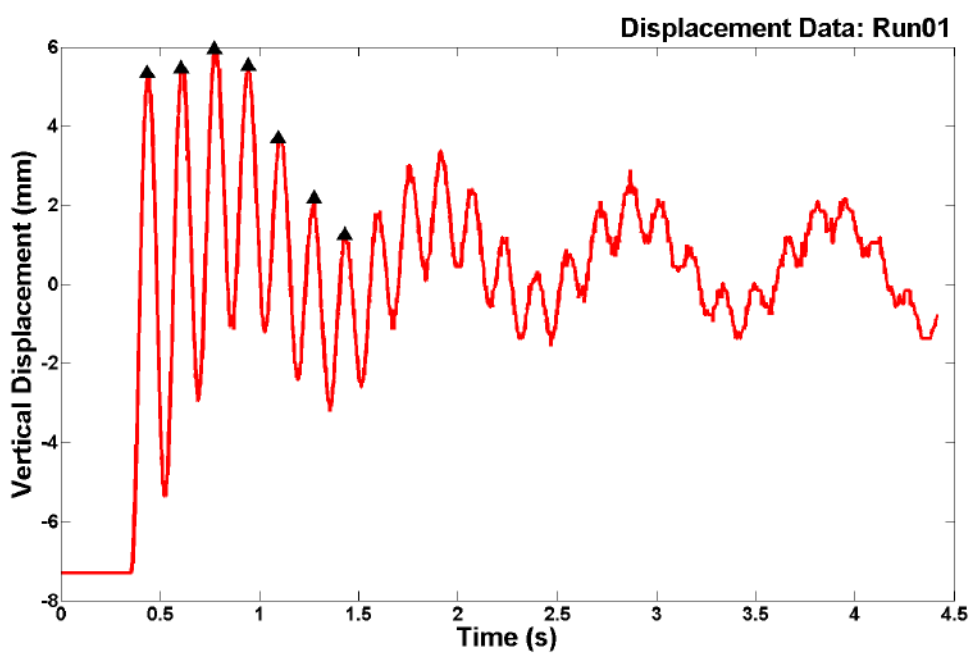


Figure 54: Peaks used for calculation of logarithmic decrement: Run01

D.2 Run02: Suspended weight 560 kg, Preload total 1050 kg

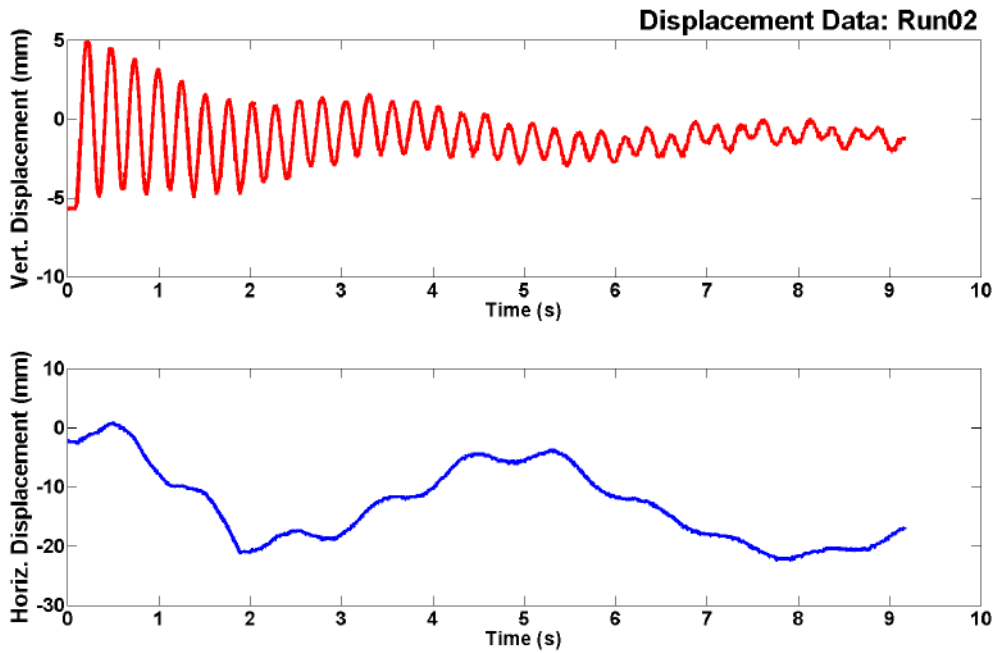


Figure 55: Vertical (top) and horizontal (lower) load displacement as calculated from motion analysis data: Run02

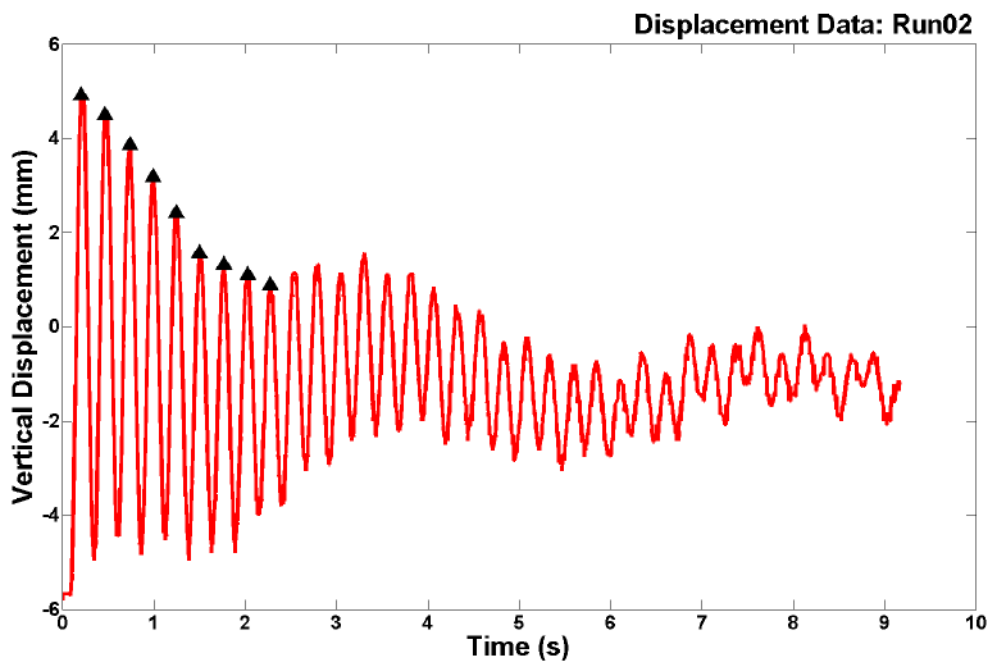


Figure 56: Peaks used for calculation of logarithmic decrement: Run02

D.3 Run04: Suspended weight 2670 kg, Preload total 3220 kg

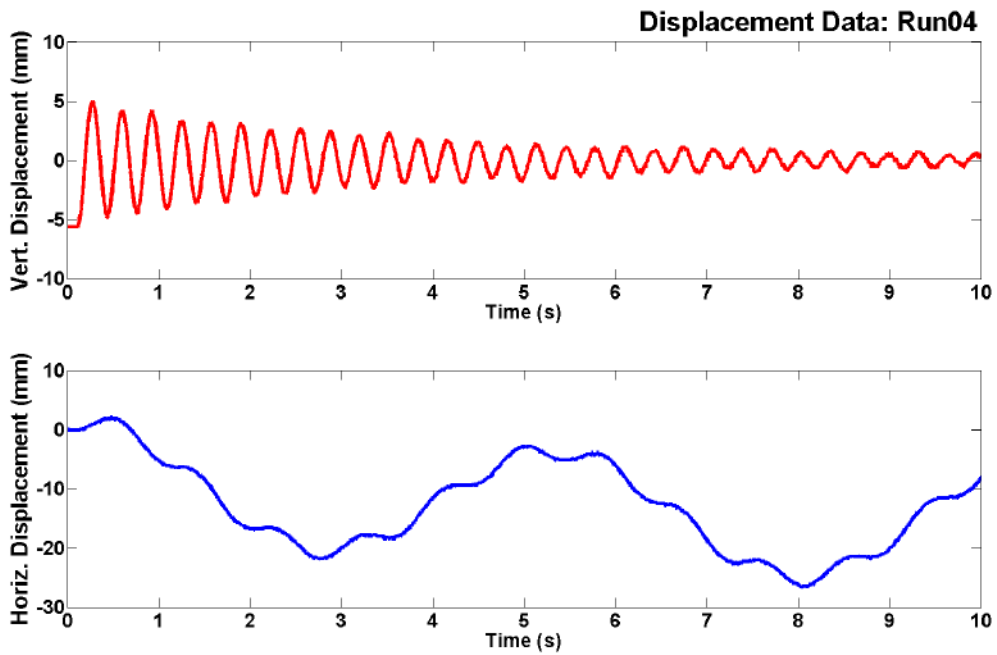


Figure 57: Vertical (top) and horizontal (lower) load displacement as calculated from motion analysis data: Run04

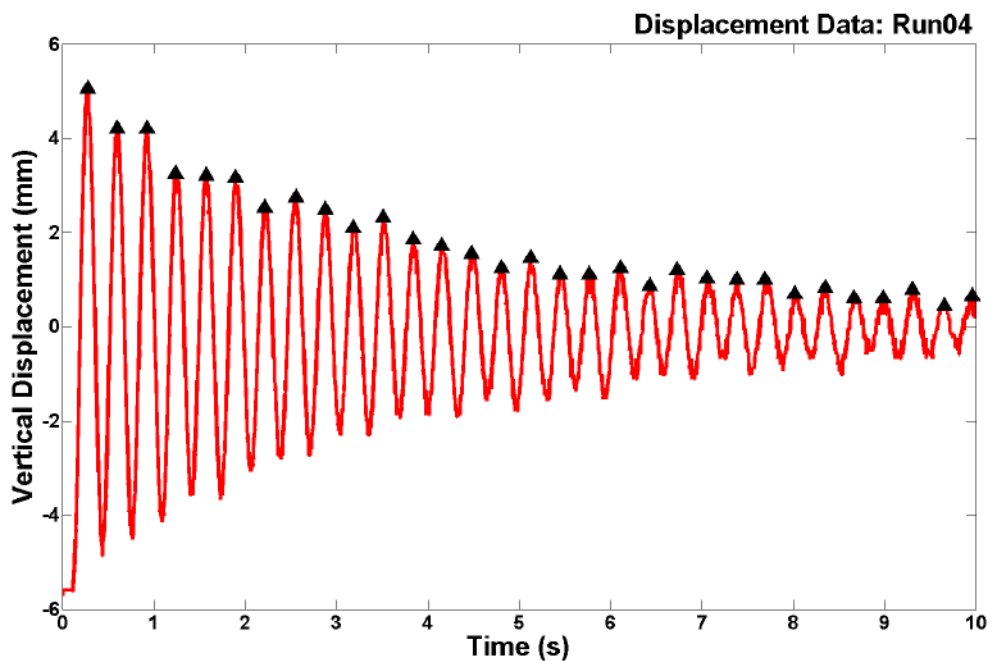


Figure 58: Peaks used for calculation of logarithmic decrement: Run04

D.4 Run05: Suspended weight 2685 kg, Preload total 3205 kg

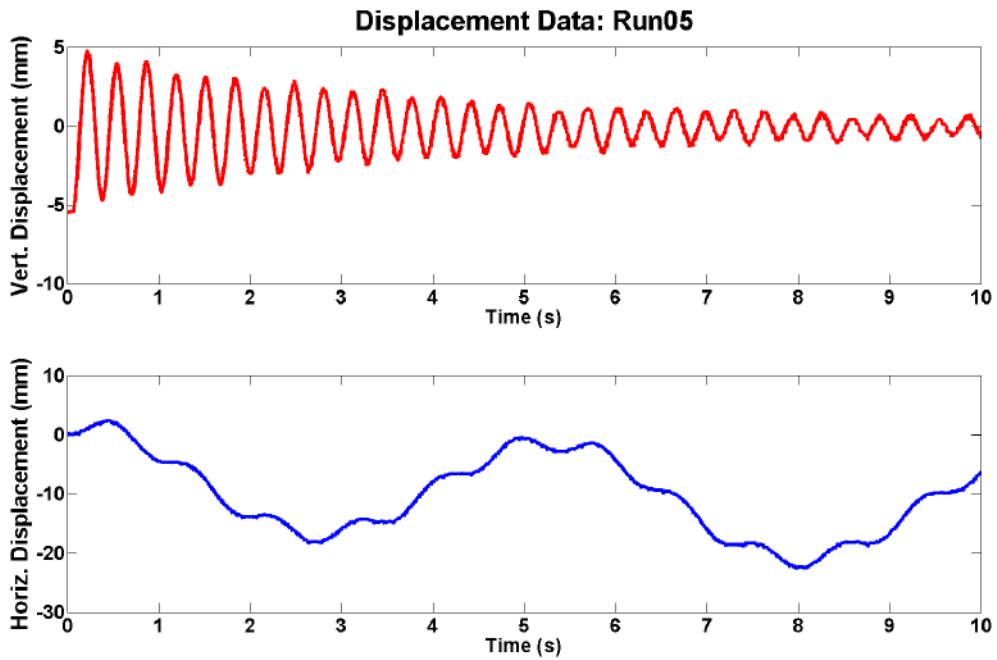


Figure 59: Vertical (top) and horizontal (lower) load displacement as calculated from motion analysis data: Run05

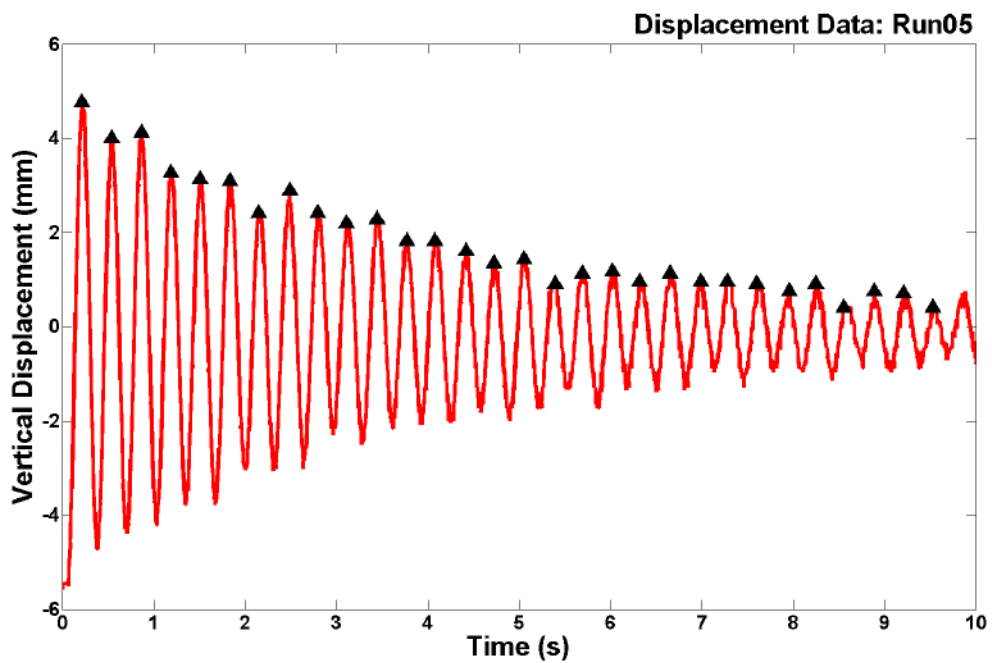


Figure 60: Peaks used for calculation of logarithmic decrement: Run05

D.5 Run06: Suspended weight 3763 kg, Preload total 4290 kg

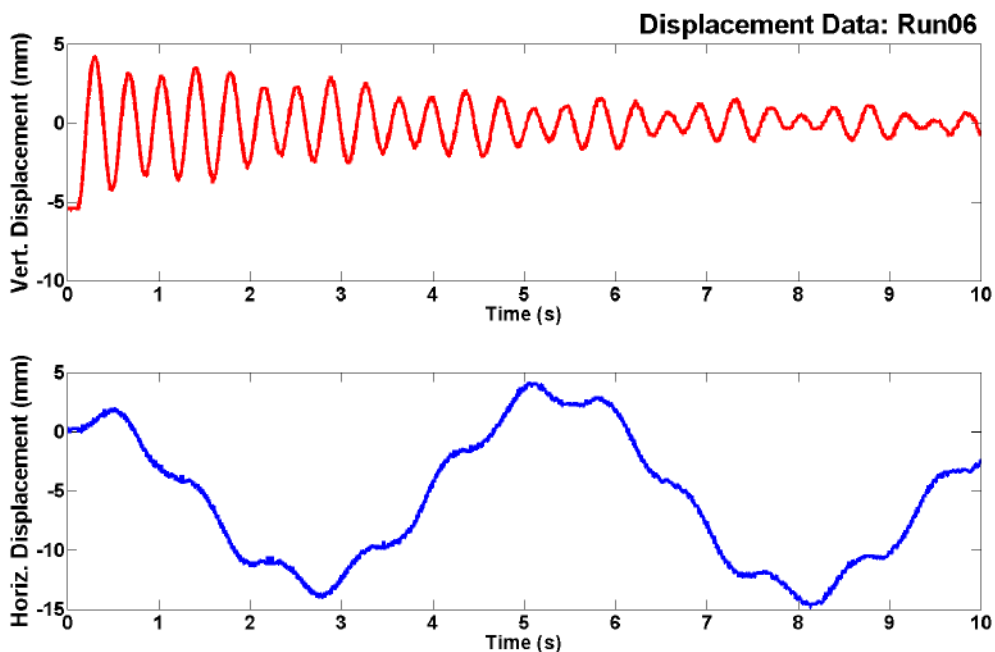


Figure 61: Vertical (top) and horizontal (lower) load displacement as calculated from motion analysis data: Run06

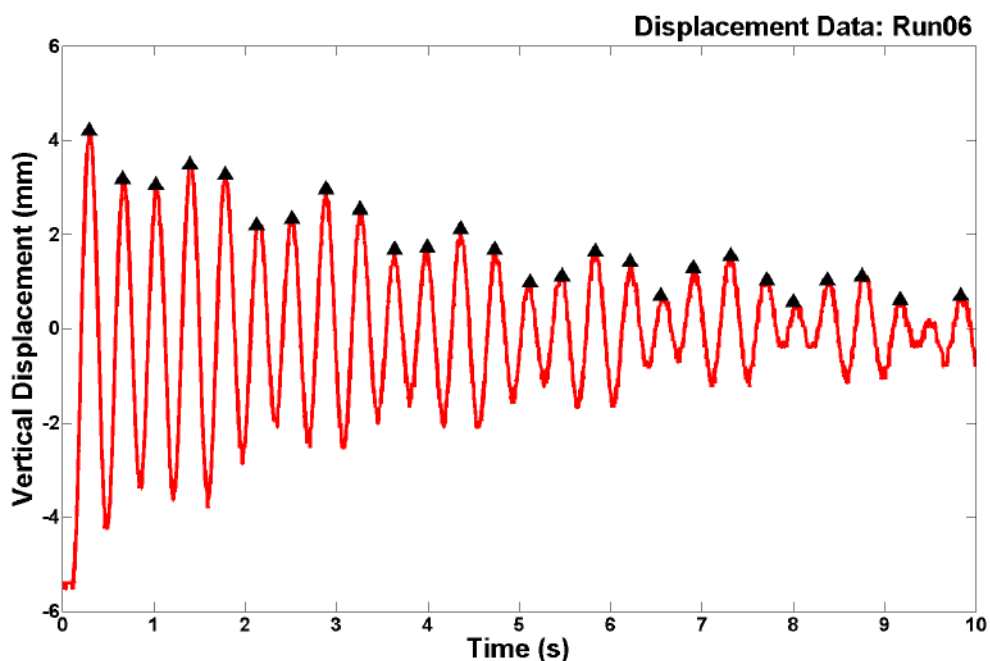


Figure 62: Peaks used for calculation of logarithmic decrement: Run06

D.6 Run07: Suspended weight 3770 kg, Preload total 4280 kg

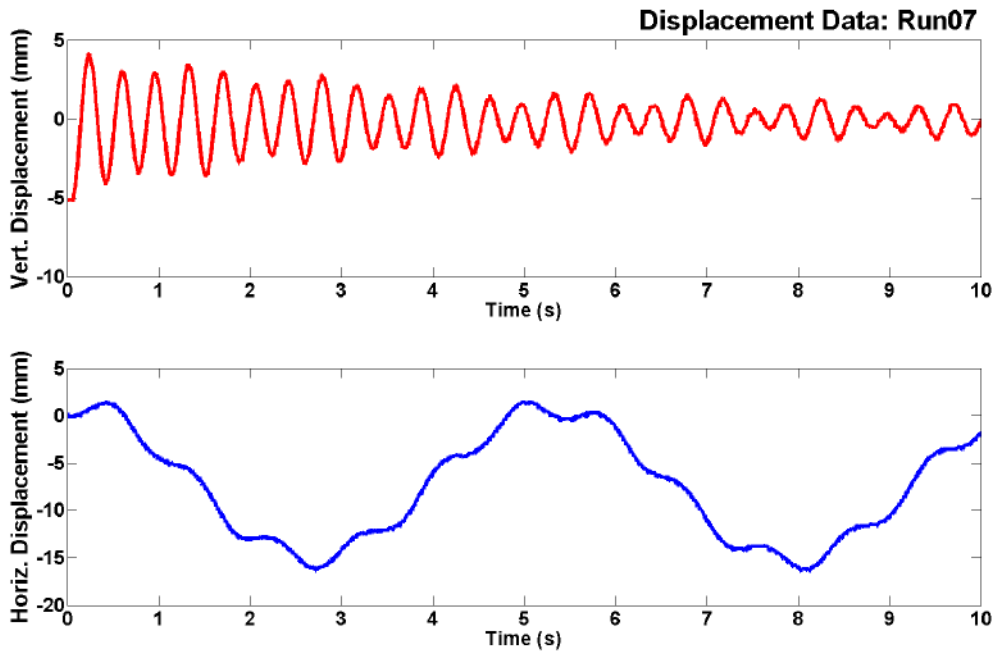


Figure 63: Vertical (top) and horizontal (lower) load displacement as calculated from motion analysis data: Run07

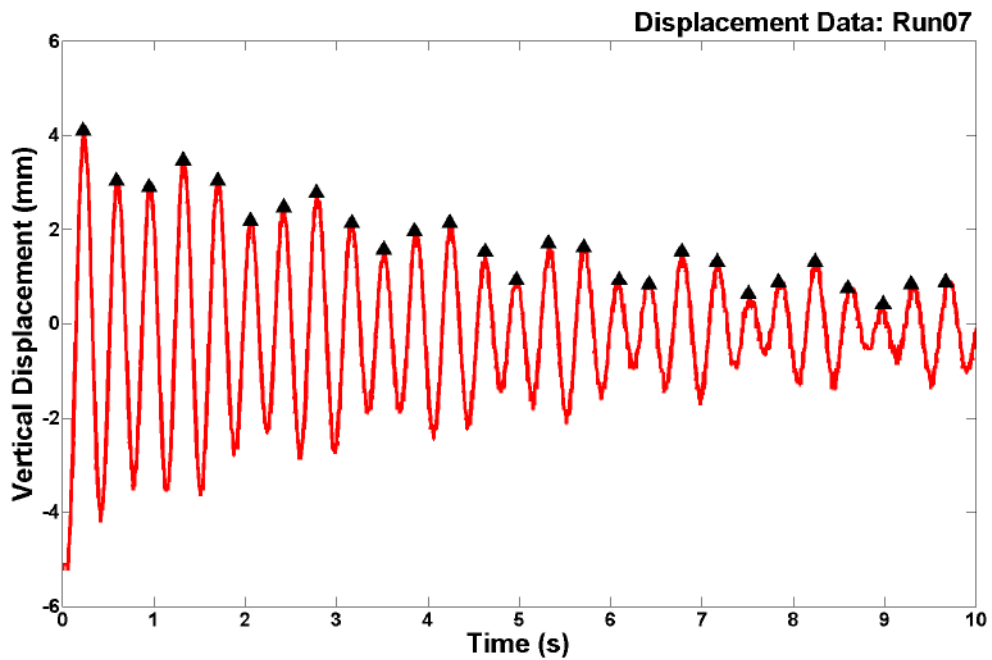


Figure 64: Peaks used for calculation of logarithmic decrement: Run07

D.7 Run08: Suspended weight 550 kg, Preload total 1045 kg

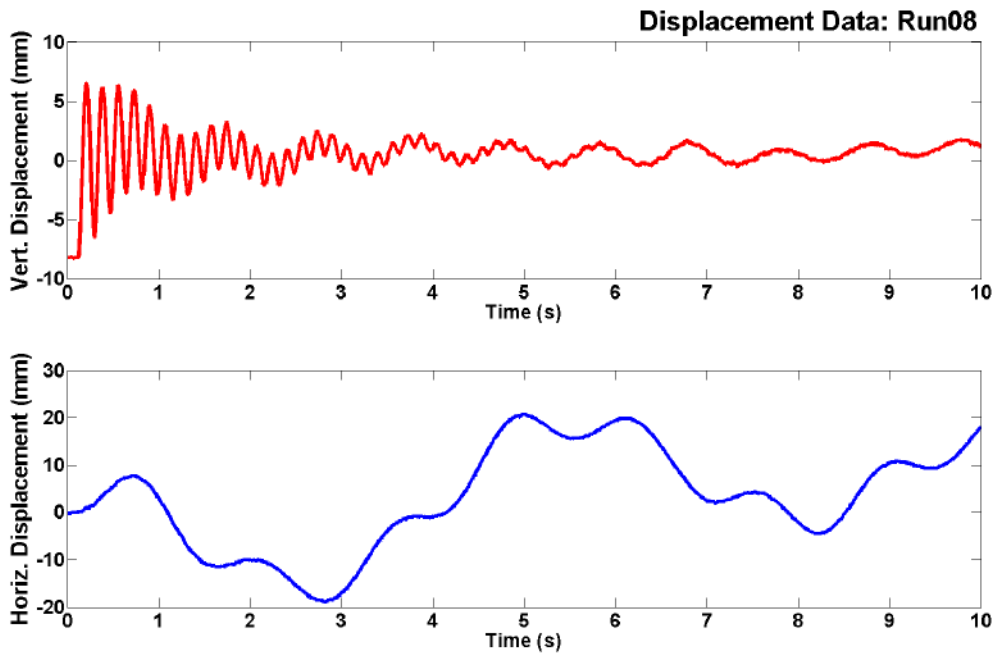


Figure 65: Vertical (top) and horizontal (lower) load displacement as calculated from motion analysis data: Run08

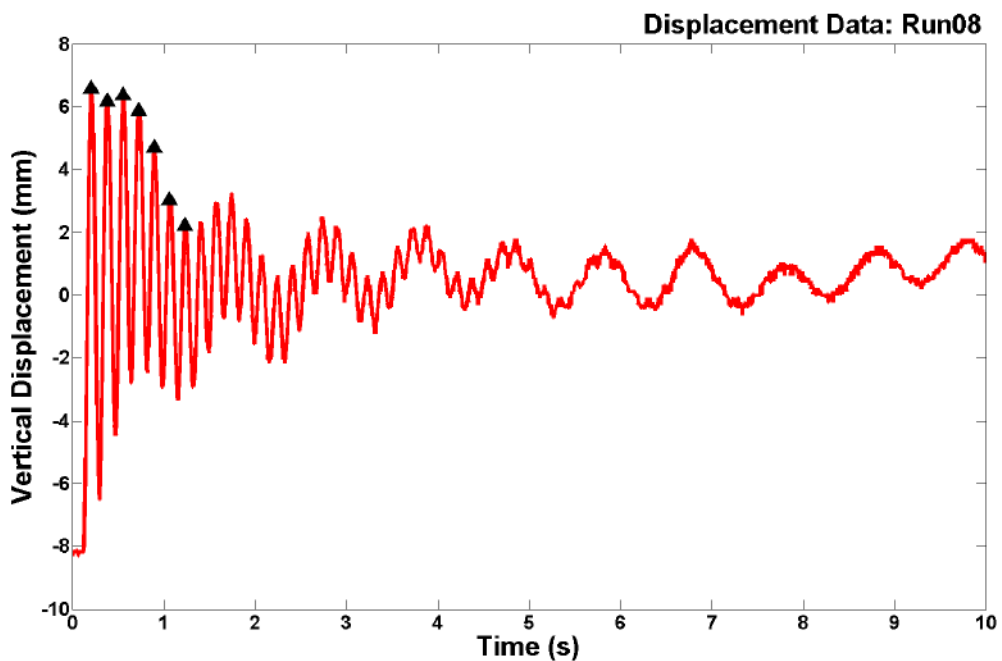


Figure 66: Peaks used for calculation of logarithmic decrement: Run08

D.8 Run09: Suspended weight 552 kg, Preload total 970 kg

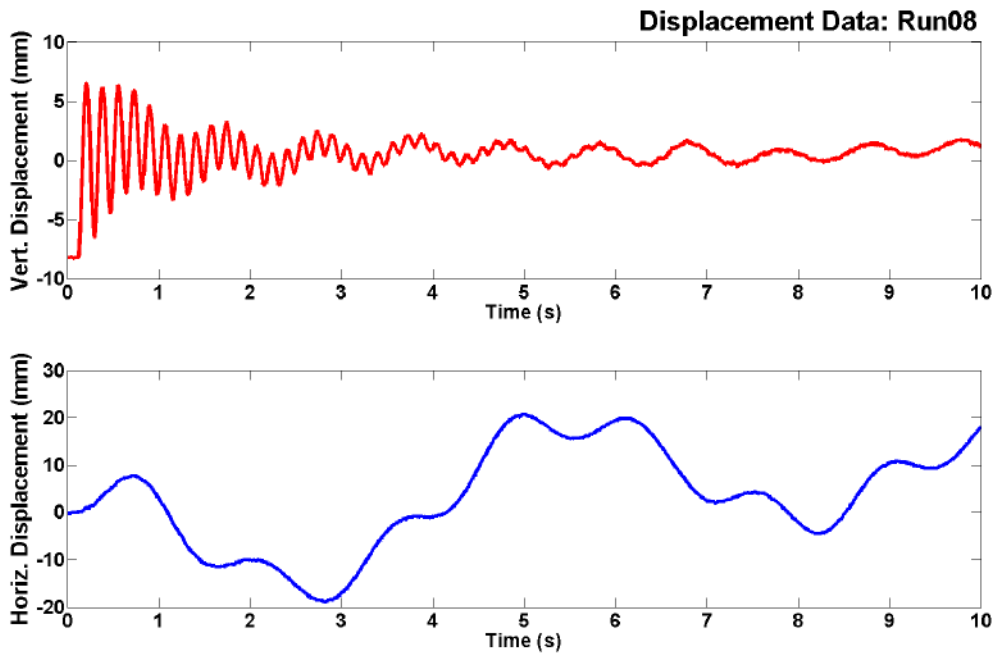


Figure 67: Vertical (top) and horizontal (lower) load displacement as calculated from motion analysis data: Run09

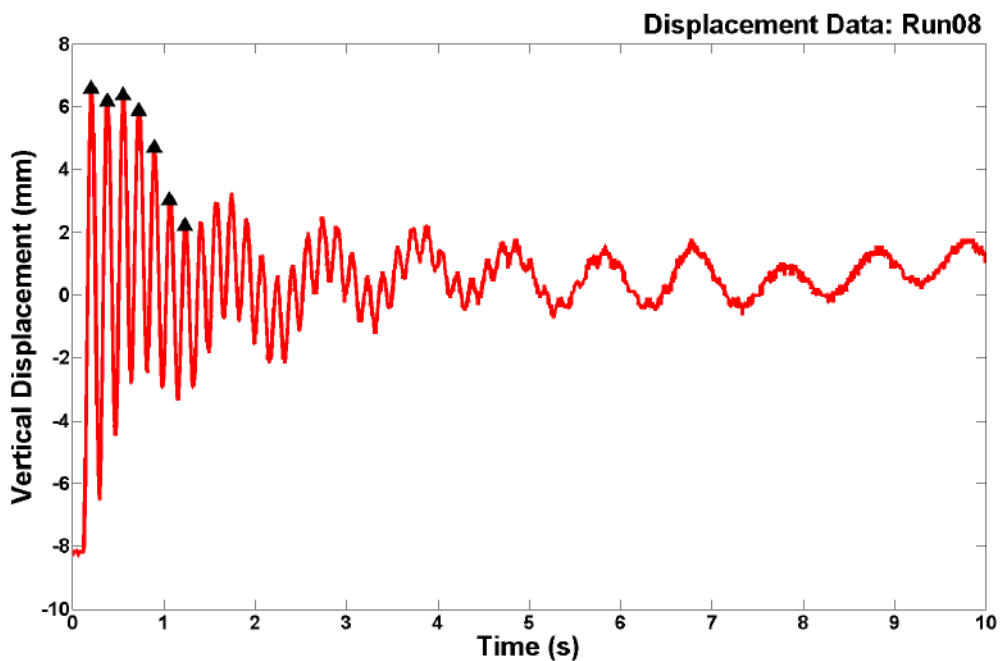


Figure 68: Peaks used for calculation of logarithmic decrement: Run09

UNCLASSIFIED

DEFENCE SCIENCE AND TECHNOLOGY GROUP DOCUMENT CONTROL DATA				1. DLM/CAVEAT (OF DOCUMENT)	
2. TITLE Mechanical Testing of Helicopter Underslung Load Equipment (HUSLE) Roundslings			3. SECURITY CLASSIFICATION (FOR UNCLASSIFIED REPORTS THAT ARE LIMITED RELEASE USE (U/L) NEXT TO DOCUMENT CLASSIFICATION) Document (U) Title (U) Abstract (U)		
4. AUTHOR(S) Kate Bourne, Keith Muller, Carl Mouser, Bruce Grigson, Jim Nicholls and Thuan Truong			5. CORPORATE AUTHOR Defence Science and Technology Group 506 Lorimer Street Fishermans Bend VIC 3207		
6a. DST GROUP NUMBER DST-Group-TN-1614		6b. AR NUMBER AR-016-835	6c. TYPE OF REPORT Technical Note		7. DOCUMENT DATE April 2017
8. OBJECTIVE ID AV14903149	9. TASK NUMBER ARM 07/038	10. TASK SPONSOR AMTDU	11. MSTC ASE		12. STC HSE
13. DOWNGRADING/DELIMITING INSTRUCTIONS			14. RELEASE AUTHORITY Chief, Aerospace Division		
15. SECONDARY RELEASE STATEMENT OF THIS DOCUMENT <i>Approved for public release</i>					
OVERSEAS ENQUIRIES OUTSIDE STATED LIMITATIONS SHOULD BE REFERRED THROUGH DOCUMENT EXCHANGE, PO BOX 1500, EDINBURGH, SA 5111					
16. DELIBERATE ANNOUNCEMENT No Limitations					
17. CITATION IN OTHER DOCUMENTS			Yes		
18. RESEARCH LIBRARY THESAURUS HUSLE, slung load, damping coefficient					
19. ABSTRACT Following on from preliminary testing in 2013, mechanical testing of the Helicopter Underslung Load Equipment (HUSLE) roundslings was undertaken in support of slung load simulation model development. DST Group conducted tensile and dynamic testing on an expired HUSLE assembly in order to identify the mechanical properties of the roundslings.					

UNCLASSIFIED